UNIVERSITY OF DEBRECEN
FACULTY OF ENGINEERING
DEPARTMENT OF
MECHANICAL ENGINEERING

Design and Analysis of a Flat Form Tool and its Clamping Device

THESIS

Tazrian Kabir Arwa
Automotive Production Process Control Specialisation

Debrecen
2025

Table of Contents

Table of notations

g_{max}	[mm]	highest radial depth
d_{max}	[mm]	highest diameter of the workpiece
d_{min}	[mm]	lowest diameter of the workpiece
γ_{xu}	[°]	tool rake angle
α_{xu}	[°]	tool clearance angle
γ_{xv}	[°]	tool construction angle
H_p	[mm]	vertical projection of the first profile point
E	[mm]	horizontal position of profile points along the rake surface.
F	[mm]	spacing between a point and the first point
G	[mm]	horizontal position of profile points along the normal plane
A_c	[mm^2]	chip cross-sectional area
V_c	[mm/s]	tangential cutting speed
V_f	[mm/s]	feed velocity
F_c	[N]	resulting cutting force
F_p	[N]	radial force
F_f	[N]	feed force
k_c	[$\frac{N}{mm^2}$]	specific cutting force

INTRODUCTION

In modern machining, the design and geometry of cutting tools play a vital part in achieving consistent and accurate work profile with repeated successions. The successful application of a flat form tool in lathe operations depends both on the tool's design and on how securely and accurately it is held during cutting opeations.

Traditional machining techniques rely heavily on multiple operations to fully achieve the desired shape for a profile that is too complex or too customized to be done at one attempt. In order to address this, this thesis focuses on the design and development of an efficient flat form tool and its corresponding clamping design. A flat form tool is a lathe cutting tool that replicates the profile of the desired workpiece. As such, it allows for complex shapes to be machined in a single pass. In this way, cycle times are significantly reduced, while maintaining consistency across parts. Flat form tool are suually suitable for serial and quantity production [1]. Besides, it is also very important to design a reliable and robust clamping system to ensure precise and consistent cuts. If the clamping system is not properly designed, improper clamping might lead to tool deflection, dimensional inaccuracy, or even tool failure.

Form tools can be divided into two categories: axial and radial cutting tools. This grouping is done based on the direction of machining [1]. The flat form tool is a radial cutting that moves perpensicular to the axis of rotation. The performane of the form tool depends on its geometry and the materials from which it is made. The most common types of materials that are used in flat form tools are high speed steel, carbide, and ceramic[2]. The advantages of this tool include shorter turning time and lower standard deviation in the produced workpieces. The flat form tool is commonly used on both conventional and CNC lathes[1].

The objective of this thesis is to design a robust flat form tool and an effective clamping device that ensures both mechanical stability and optimized cutting performance. Initially, theoretical calculations and constructional evaluation are done to ensure the validity of the design. Furthermore, simulations on finite element analysis software, ANSYS are also carried out to ensure that the final design is able to bear operational loads and produce the desired profile accurately. The findings are intended to serve as a basis for future improvements in tool design and clamping systems.

1 Literature Review

1.1 Origins of the Lathe Machine

The lathe, a core machine tool, lies at the heart of industrial manufacturing and production. If we dig deeper into history, we will find that 3000 years ago, the Egyptians were among the first to use a form of lathe technology. It was discovered that the Egyptians craftsmen used to operate primitive **bow lathes**. Two people would have to operate this lathe, where one of them would hold the cutting tool and the other would rotate the workpiece back and forth by pulling on a cord or a thong [3], allowing them to shape wood and soft materials [4].

The next major evolution, which did not come until the Middle Ages, is the evolution of the **spring-pole lathe** which became widespread among the Europeans. A cord ran from the pole, around the workpiece and to a foot pedal, allowing craftsmen to rotate the workpiece back and forth by stepping on the foot pedal and releasing it [3]. During the late Middle Ages, to eliminate the tiresome manual foot work, water-powered lathe was introduced known as **hydrokinetic lathe**. This lathe converted the back-and-forth motion of the spring-pole lathe into continuous rotational motion as the waterwheel, which was placed in a flowing river or a mill system, transferred rotational energy to the lathe when water flowed over it [4,5].

Steam powered lathe was introduced during the Industrial Revolution, a major leap in lathe technology. This lathe utilised a steam engine to drive its motion, allowing it to operate at higher speeds and greater efficiency [4]. However, this lathe started to get replaced after the invention of the electric motor. This is because the electric motors were installed in the lathe, making it an **electric powered lathe**. This shift in mechanism not only improved efficiency but also provided with more reliable and consistent power. This eventually led to smooth, uniform motion for machining, enabling higher accuracy [6].

Finally, in the latter half of the 20th century, **Computer Numerical Control (CNC) lathes** were introduced. CNC lathes are computer-controlled machines that allow us to input pre-programmed tool movements, significantly improving precision and automation. As such, CNC lathes have become indispensable in modern workshops that require high precision and complex machining operations [4,6].

1.2 Overview of the Lathe Machine

The mother of all machines, lathe, works by eliminating the undesired materials from the workpiece in the form of chips and giving it the required size and shape. In the lathe machine, the workpiece rotates, while the cutting tool remains fixed or moves linearly to give the workpiece its required shape [7]. The various parts of a lathe machine are shown in Figure 1.

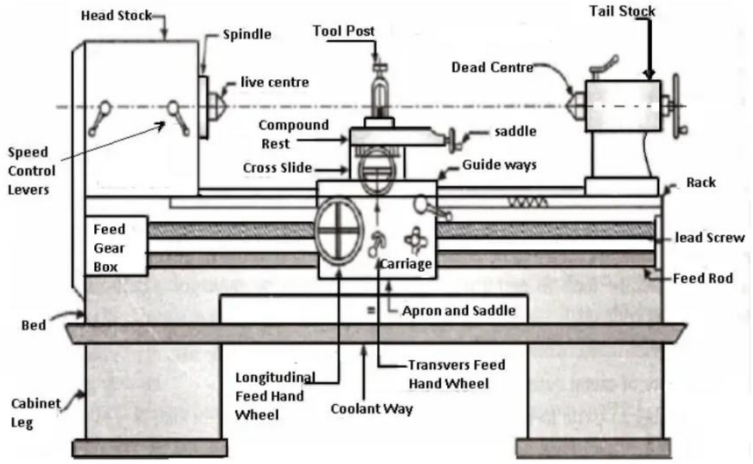

Figure 1: Different parts of a lathe machine [8]

Lathe comes in a variety of sizes depending on their applications. However, the principle of working is the same for all types of lathes. The different kinds of lathes are:

Engine Lathe: Engine lathe is the most common and widely used lathe machine [9].

Speed Lathe: As the name suggests, the speed lathe operates at a high speed, ranging from 1200 rpm to 3600 rpm for light duty operations [9].

Bench Lathe: This lathe is the smaller version of the engine lathe, commonly used for light duty machining [9].

Tool Room Lathe: Tool room lathe is a high precision lathe and is mostly used for manufacturing accurate machining components, dies, tools etc. [9].

Capstan and Turret Lathe: Designed specifically for mass production and production of similar parts, Capstan and Turret lathe is an advanced version of engine lathe [9].

Computer Numerical Control (CNC) lathe: A CNC lathe is a computer-controlled lathe that needs computer coding, specifically G-code and M-code to carry out machining. Since the movement is controlled by codes, it's a very high-speed, precise machine.

1.3 Different Lathe Operations

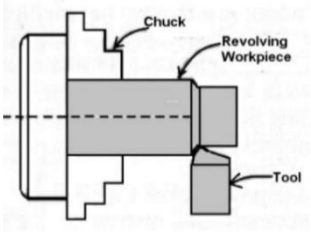

Figure 2: Turning [10]

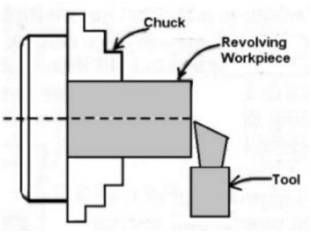

Figure 3: Facing [10]

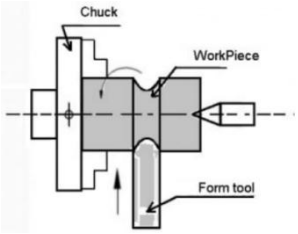

Figure 4: Forming [10]

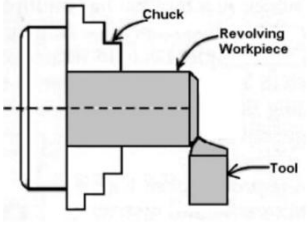

Figure 5: Chamfering [10]

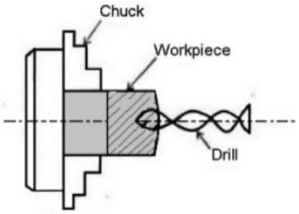

Figure 6: Drilling [10]

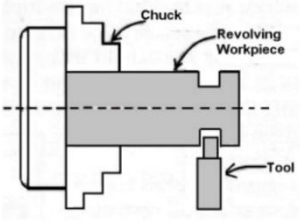

Figure 7: Grooving [10]

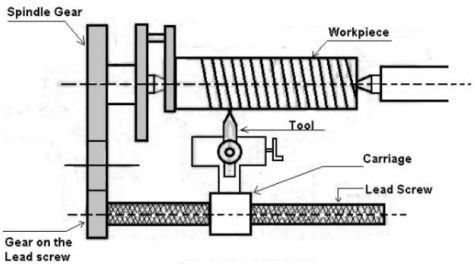

Figure 8: Threading [10]

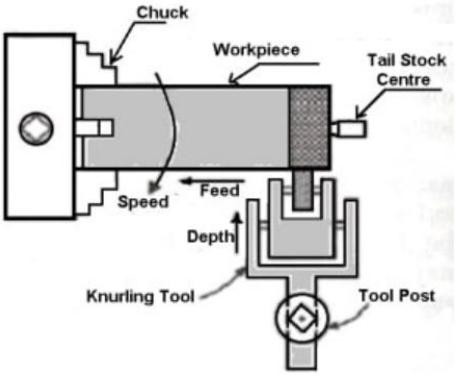

Figure 9: Knurling [10]

1.4 Overview of the Form Tool

A form tool is a specialised cutting tool of a lathe machine which is used in machining complex profiles. The component manufactured by the forming operation usually takes the shape of the forming tool. One of the advantages of form tool is that it cuts the entire profile in a single pass making it faster than traditional cutting tools. This tool is used in serial and quantity production where repetitive profile accuracy and efficiency are required [1].

Since form tools undergo heavy cutting loads, the following are the materials with which form tools are manufactured to maintain profile accuracy for repeated operations: -

High-Speed Steel (HSS) Form Tools: HSS form tools are widely used for their toughness and resistance to wear. They can withstand high temperatures, allowing for faster cutting speeds [2].

Carbide Form Tools: Form tools made of carbide, especially tungsten carbide (tungsten-carbon) and cemented carbide (tungsten-carbon-cobalt), are well known for their exceptional hardness and their ability to retain a sharp cutting edge at high temperatures [2,11].

Cobalt Form Tools: Combining thermal resistance of carbide with the toughness of high-speed steel, the carbide tools are ideal for machining work that require both durability and the ability to handle high temperatures [2].

Diamond Form Tools: For ultra-precision machining tasks, particularly for hard-to-cut materials, diamond form tools are a great choice. As the name suggests, this form tool's cutting edge is made of diamond [2,12].

Ceramic Form Tools: Although form tools made of ceramic are more brittle than other types, however, they are extremely hard and resistant to wear. They are preferred for high-speed machining of hard materials [2,12].

However, form tools made of HSS, and carbide are mostly in practise.

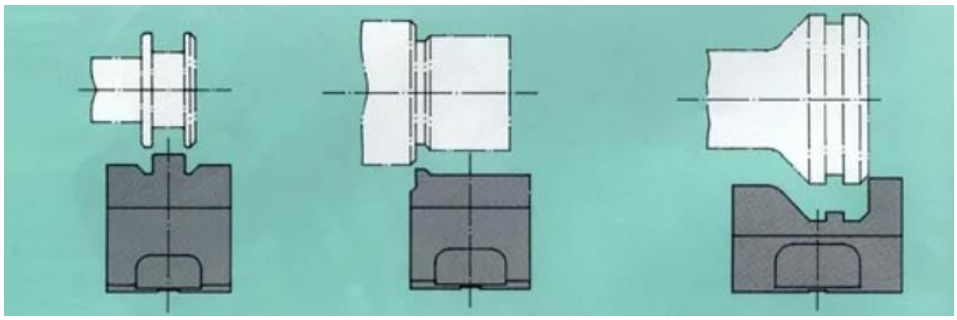

Figure 10: Different types of form tools [11]

The design of a form tool is pivotal to ensure effective material removal, profile accuracy and tool life during machining. Following are the design principles of a form tool that will make sure that the workpiece is efficiently machined to get the desired result: -

- Selection of the right material for the cutting tool which will be compatible with the workpiece material [2,13].
- Determination of the overall dimensions like the length, width, thickness of the tool, considering the part that needs to be manufactured as well as the machine setup [2,13].
- Calculation of the shape and geometry of the cutting edge of the tool that will reproduce the desired profile on the workpiece [2].
- Preparation of the detailed technical drawing of the cutting tool showing all the critical dimensions, angles and tolerances [2,13].

There are several advantages of using form tool.

- As the shape of the form tool corresponds with the profile of the workpiece, it ensures high precision and accuracy in the produced parts [2].
- Use of form tool minimizes the machining time and speeds up the production process since desired profile is attained in a single pass [2].
- Form tools reduce the need for tool changes by attaining the desired shape in one pass [2].
- Since a single pass is needed to shape a workpiece, it decreases downtime for tool replacement as well as reduces wear and tear on the machinery [2].
- A wide variety of profiles can be manufactured using custom form tools [2].
- Constant adjustment is not needed while machining using form tools, making them very handy and user friendly [2].

The following could be the disadvantages of using form tool: -

- Since form tools are designed for a specific shape or profile, it makes them unsuitable to use for different purposes.
- Form tools are sometimes custom made, so the initial cost could be high.

1.5 Classification of the Form Tool

Form tools are generally classified into three groups according to their cross section: -

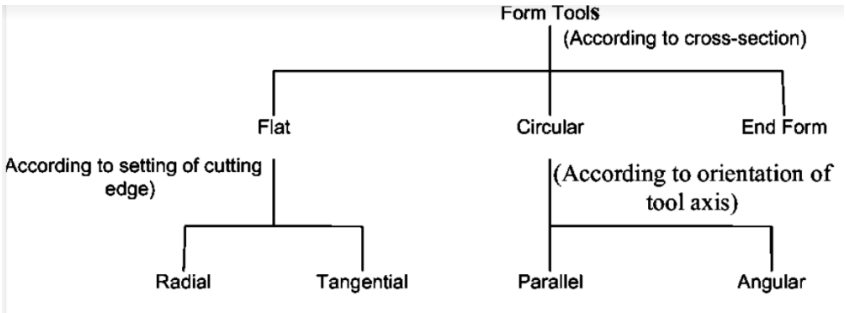

Figure 11: Classification of form tools [14]

Flat Form Tool: In a flat form tool, the cross section is typically square or rectangle, providing necessary strength and support during the cutting operation. Form tools are positioned centrally to ensure that the tool profile is perfectly transferred to the workpiece [14]. To provide smooth chip flow, the rake surface of the flat form tool is flat. Besides, to maintain consistent clearance during cutting, the flank surface of the flat form tool is made to match the cylindrical surface of the rotating workpiece. The clearance angle of a flat form tool is usually set to be between 25 to 30 degrees to make sure the tool does not rub against the workpiece. However, the rake angle depends on the material being machined [13].

The flat form tool is classified into two types based on the direction of the tool movement- radial and tangential [13]. In the radial feed system, the tool is set in such a way that the cutting motion is directed inward or outward along the radius of the working piece [13]. This setup ensures that the cutting edge maintains uniform contact as it feeds into the material creating the desired profile on the workpiece. However, in the tangential feed system, the form tool is tangential to the surface of the rotating workpiece [13]; meaning the tool moves parallel to the outer surface, along the length of the cylindrical workpiece.

Figure 12: Flat Form Tool [15]

Circular Form Tool: As evident from the name, the shape of the circular form tool is circular. In circular form tools, the flank face is designed symmetrically around the tool's axis, ensuring consistent shape across the contact area. Circular form tools are positioned in such a way that the centerline of the tool is offset from the center of the machine spindle. This setup ensures producing an effective front clearance angle at the cutting edge. By setting the tool axis above the work axis, the clearance angle is obtained in a circular form tool. The clearance angle of a flat form tool is usually set to be between 10 to 12 degrees [13].

The circular form tool is classified into two types based on the orientation of tool axis- parallel and angular. In case of parallel setup, the tool axis is set parallel to the workpiece axis, while for angular setup, the tool axis is set at an angle to the workpiece [14].

Figure 13: Circular Form Tool [16]

End Form Tool: An end form tool is a type of form tool which is used to shape the end of the tubes. This tool is designed to produce shape at the end of the tubes which will fit other parts. Tube diameters are expanded, reduced and calibrated using this end form tool [17].

Figure 14: End Form Tool [18]

1.6 Overview of the Design of Clamping Device

In any manufacturing setup, the system of part production typically includes machine tools, production tools, workpieces, measuring instruments, and specialized devices. Among these, to keep the cutting tool aligned with the workpiece during the manufacturing process, a clamping device is an indispensable mechanical system to secure the cutting tool firmly in place. The functions of the clamping device are-

- To ensure that the tool remains fixed, stable and accurately positioned, resisting movements caused by cutting forces and vibrations [19].
- To enable quick and efficient tool changes, especially in high volume and automated production settings [19].

To ensure complete positional accuracy and eliminate tool movement during operation, the six-point location principle is applied to clamping device. This

setup ensures that all six degrees of freedom are controlled, providing maximum repeatability and rigidity during forming operations [19]. Three base supports are used to fix the tool in vertical direction, two side locators constrain lateral movement and one end stop restricts longitudinal displacement.

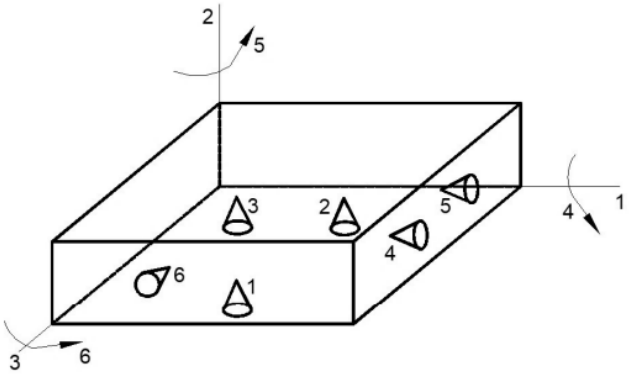

Figure 15: Illustration of the six-point standard [19]

The design of a tool clamping device must incorporate effective locating strategies to ensure rigidity and accuracy. There are three forms of location used for tool holding- plane, concentric and radial [19].

a) Plane location: Plane locators are used to support the flat base of the form tool [19].
b) Concentric location: Concentric locators are used to support the tool from the central axis [19].
c) Radial location: Radial locators are used to prevent the tool from rotating about its own axis during operation [19].

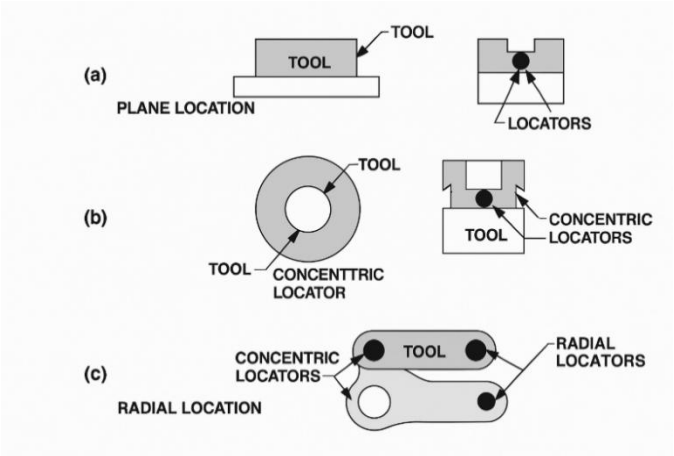

Figure 16: The three forms of location [20]

Based on the number of degrees of freedom constrained, the positioning of a tool or workpiece can be classified into three categories:

- **One directional determination:** In case of one directional determination, the tool is stabilized in one plane using a three-point locating system, which fixes three degrees of freedom, typically vertical translation and tilting about two axes [19,20].
- **Two directional determination**: In this case, five degrees of freedom are restricted using two locating elements that define two perpendicular planes. This setup is typically used when two dimensions need to be controlled simultaneously during a single manufacturing step [19,20].
- **Three directional determination (total determination)**: When it comes to three-directional determination, all six degrees of freedom are fully constrained. This method is applied when three critical dimensions must be maintained within a single machining [19,20].

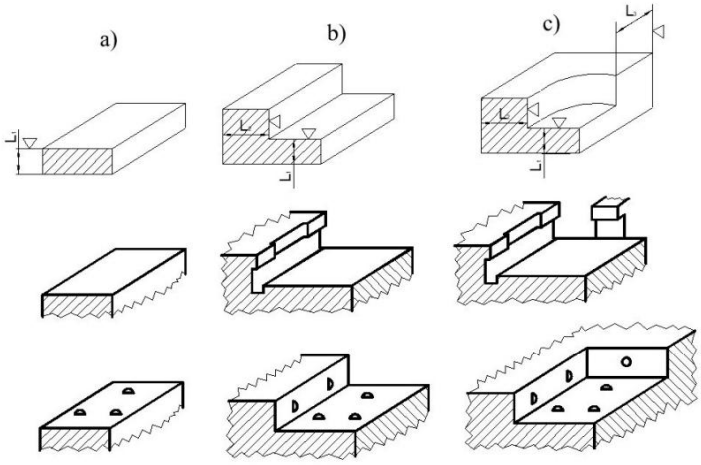

Figure 17: The three types of position determination [19]

Furthermore, there are also different types of mechanical supporting elements used to hold a tool from below to maintain stability and accurate positioning. They serve as the theoretical fixed points in clamping design [19].

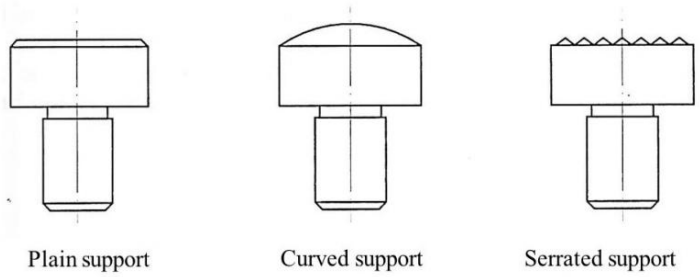

Figure 18: The variety of supporting elements [19]

Figure 19 shows how a support element is installed in a clamping system.

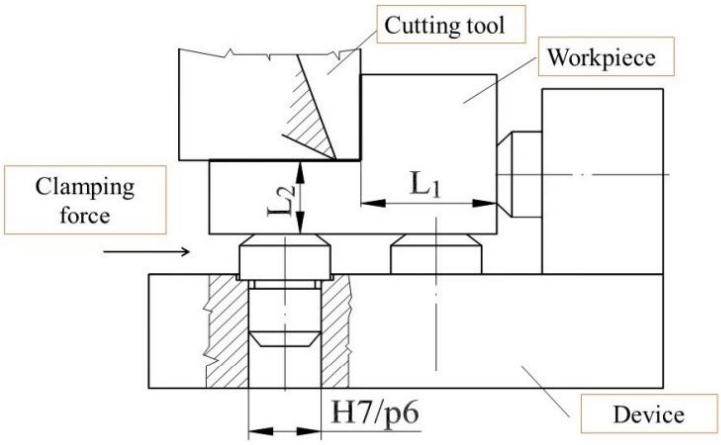

Figure 19: Process of installing a support system [19]

Figure 20 illustrates how the accuracy of surface positioning depends on the proper arrangement of supports and locators. Here, the reference surface is considered to be D.

When the tool is evenly supported (case a), the reference surface remains stable and accurate. However, the tool expeiences uneven support in case b, since only one portion of the surface is in contact. This phenomenon causes the tool to shift or vibrate during operations. As a result, there is a possibility of deviation of the desired profile at the end. Furthermore, case c shows a more critical issue, which is tilting of the tool. The tool is not seated parallel to the surface of the workpiece which might lead to angular misalignment. This distorts the cutting geometry affecting the final accuracy of the shape.

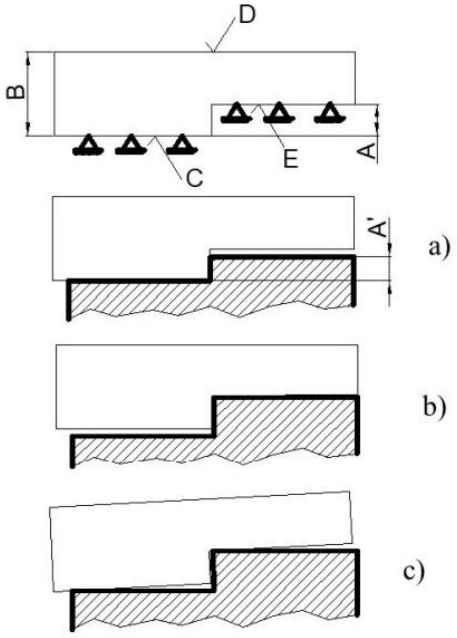

Figure 20: Depiction of accuracy of surface positioning [19]

1.7 Finite Element Analysis (FEA) in Tool Design

During cutting process, a cutting tool is subjected to multi-axial stresses [21]. So, to assess structural performance and operational reliability of a cutting tool, Finite Element Analysis (FEA) is an imperative method in modern mechanical design. This simulation-based approach helps to analyze stress distribution, deformation behavior, fatigue analysis, thermal analysis, factor of safety etc. under realistic loads typically encountered during lathe operations [22].

To carry out the finite element analysis, a detailed 3D model of the cutting tool is created using software like Solid Edge, Solid Works, CATIA etc. The 3D model is then imported into FEA software i.e. ANSYS. This software is then used to carry out static and dynamic analysis under varying loads and conditions. However, to carry out an accurate FEA, it is essential to define the correct material properties i.e. Young's Modulus (E), Poisson's Ratio (ν), Density (ρ), Yield Strength etc [23].

The foundation of FEA is to break down the cutting tool into many small parts called the elements. The elements are connected by nodes. These nodes and elements form a mesh- a simplified representation of the object. The mesh allows computers to predict how the object reacts when forces or stresses are applied [22]. Each element is treated as if it's in equilibrium [21]. In this way, we can calculate how stress and force are distributed across the entire cutting edge. Following this, the boundary conditions are applied. After the boundary conditions are applied, the next step is to assign the external loads to the model i.e. forces, pressures, temperatures, or displacements, depending on the type of analysis performed. Thereafter, the software does calculation and analysis, and yields results for displacement, stress, strain, and temperature distribution throughout the model [23]. These results help in understanding the mechanical behavior of the cutting tool under realistic working conditions.

There are several advantages of carrying out the FEA to simulate machining processes mentioned by Cakir and Isik (2005).

- FEM allows material behavior to change dynamically during the simulation. This is important because materials behave differently when deformed rapidly or at high temperatures (which is common in machining).
- Accurate modelling of chip-tool interaction, capturing both sticking and sliding effects.
- The capability to handle complex, non-linear boundaries- such as the changing shapes and curving boundaries (like the flowing chip).
- FEM gives both macro-level results (overall cutting forces and chip formation) as well as micro-level results (stress concentrations, heat zones, tool wear zones etc).

Figures 21, 22, 23 and 24 show the possible outcomes that can be obtained from doing Finite Element Analysis.

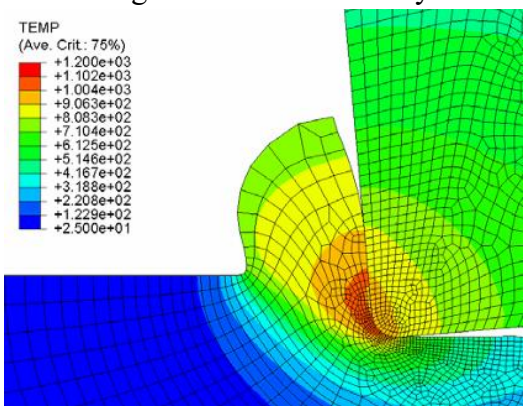

Figure 21: Temperature distribution of a cutting tool when the cutting depth is 0.25 mm [24]

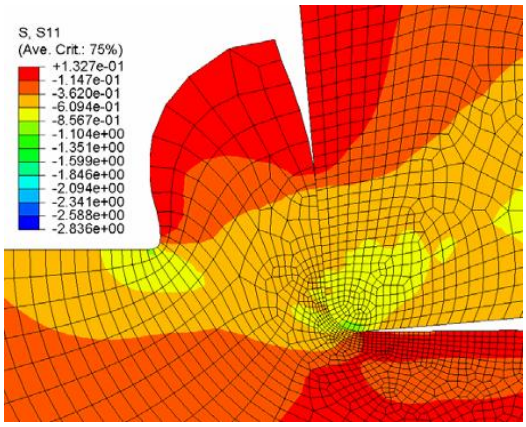

Figure 22: Stress distribution in the horizontal cutting direction of a cutting tool [24]

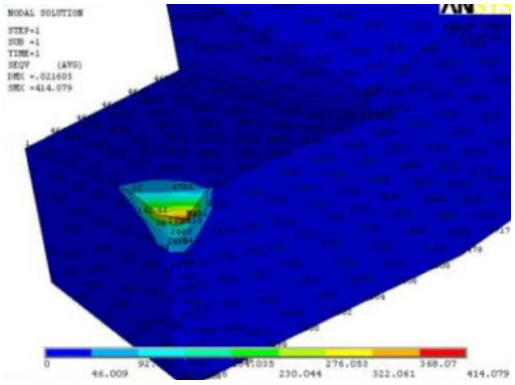

Figure 23: Von mises stress distribution of a cutting tool [25]

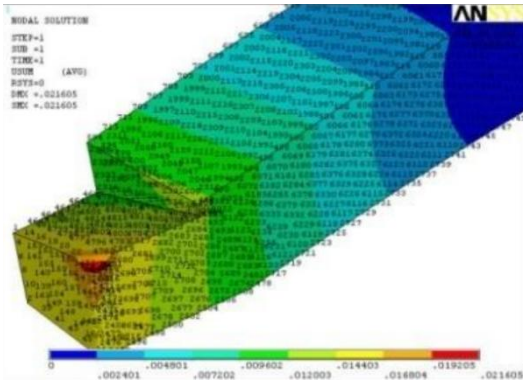

Figure 24: Deformation distribution of a cutting tool [25]

Figure 21 shows the temperature distribution in the cutting tool when the cutting depth is 0.25 mm. The highest temperature zone is seen to be at the cutting edge caused by maximum friction and deformation.

Stress distribution can be seen in Figure 22 indicating the highest stress level near the cutting edge.

Figure 23 shows the Von mises stress distribution which is a critical factor in predicting yielding (beginning of plastic deformation) under complex loading. It identfies regions where the tool is most likely to fail due to high mechanical loads. In our case, it's the cutting edge of the tool.

Total deformation is seen in Figure 24. Again, the highest deformation is at the cutting edge, confirming it as the most stressed and thermally affected region. The colour gradient shows how the deformation gradually reduces further from the tip.

2 Determination of the Form Tool Profile using Mathematical Methods

2.1 The geometric establishment of the workpiece

In order to design an effective flat form tool, it is essential to first establish the geometric profile of the workpiece. This includes the critical contours, radii, steps, chamfers, tapers or grooves that must be replicated during machining. The profile geometry is defined using dimensional parameters, which serves as the first of the subsequent tool design calculations.

In this paper, we considered the workpiece to be 120 mm in length, consisting of multiple features including chamfer, taper and a curved contour defined by a radius of 50 mm. The profile started with a chamfered section at one end, followed by a cylindrical portion of 25 mm length and 55 mm diameter. This was then followed by a curved transition created by a fillet of radius 50 mm, leading into a tapered section of the same diameter (55 mm) with a length of 30 mm. Finally, the workpiece ended in a larger cylindrical portion of 60 mm and remaining length of 40 mm.

A schematic profile of the desired workpiece can be shown in Figure 25.

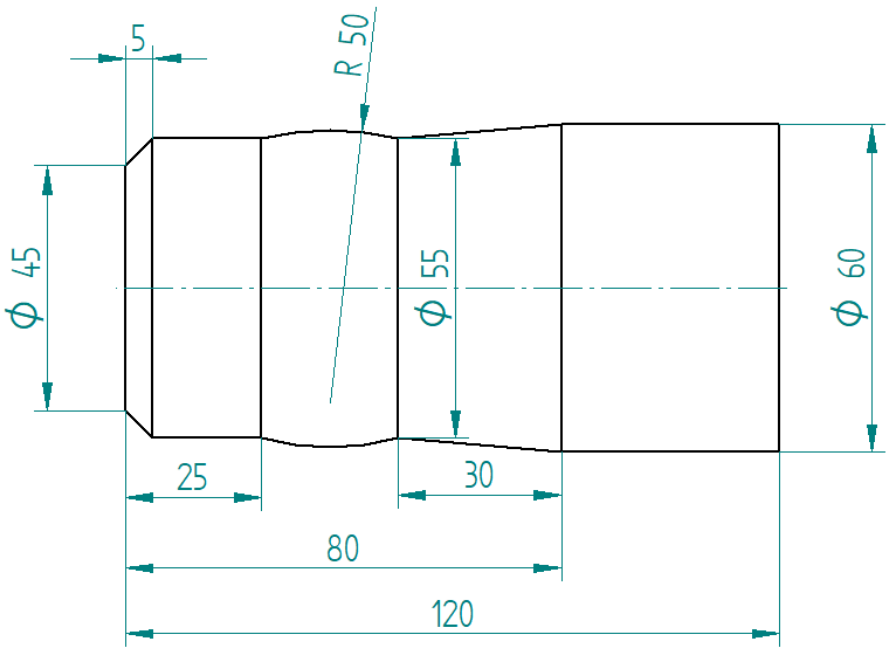

Figure 25: Technical drawing of the desired workpiece

A 3D representation of the workpiece is shown in Figure 26.

Figure 26: An isometric view of the workpiece

To determine the outside section of the cutting edge, machining allowances must be considered. As illustrated in Figure 27, such an allowance is provided to facilitate the finishing operation on the face surface of the workpiece. In this configuration, two additional edge sections: 1' and 1'-1" are introduced. The 1' section added to the chamfered section, which is inclined at an angle of 15°, and its length is determined based on the required allowance. Meanwhile, the length of 1'-1" section is generally selected within the range of 2 to 3 mm [26]. It can be seen in Figure 27 that the total edge length is greater than the formed length.

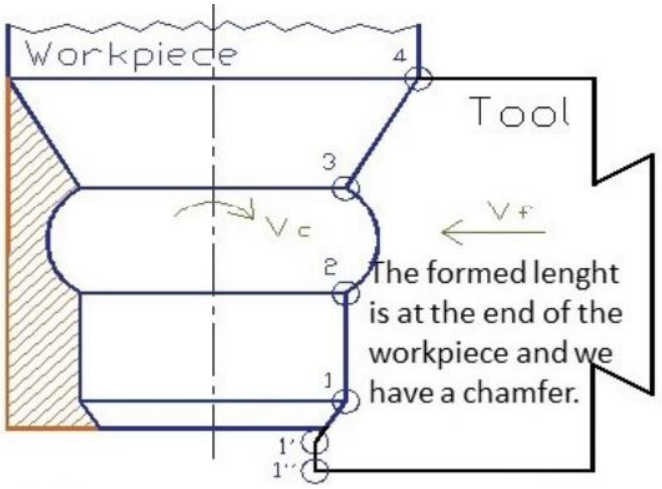

Figure 27: Determination of outside section of cutting edge [26]

The first step of the calculation method is the determination of the highest radial depth, g_{max} of the flat form tool. It is the highest depth of material that is to be removed from the workpiece. It can be calculated as half the difference between the maximum and minimum diameters of the desired workpiece. This value determines how far the tool must move inward from the surface. It also serves as a primary design parameter for selecting the tool dimensions.

$$g_{max} = \frac{d_{max} - d_{min}}{2} \qquad (1)$$

d_{max}: the highest diameter of the workpiece

d_{min}: the lowest diameter of the workpiece

For our given workpiece, d_{max} = 60 mm and d_{min} = 45 mm. Incorporating these values into the formula, we get g_{max} = 7.5 mm. This result represents the deepest radial position that the form tool must reach to achieve the required profile.

The external geometry of the flat form tool, including the maximum radial depth g_{max}, and its corresponding parameters and dimensions is presented in Figure 28. This diagram serves as a reference for interpreting the values listed in Table 1.

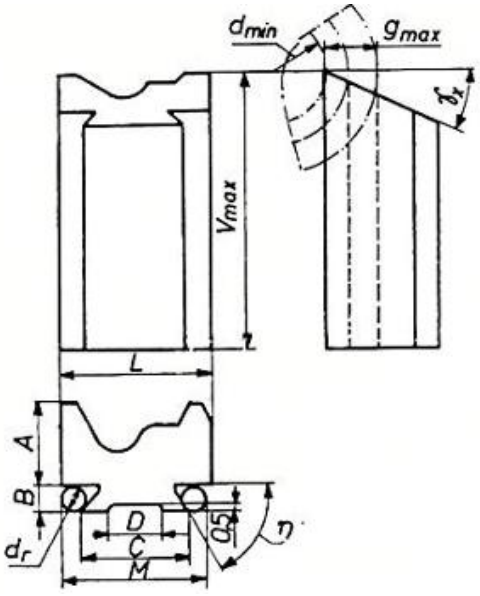

Figure 28: External geometry of the tool [1]

Referring to Figure 28, the main dimensions of the form tool can be selected from the standard tool sizes listed in Table 1.

g	The main sizes of the tool						The total size of the *M* clamping part			
	A	*B*	*C*	*D*	*V*	*r*	d_{r1}	M_1	d_{r2}	M_2
until 4	9	4	15	7	75	0.5	4	21.31	3	18.577
4...6	14	6	20	10	75	0.5	6	29.46	4	24
6...10	19	6	25	15	75	0.5	6	34.46	4	29
10...14	25	10	30	20	90	1	10	45.77	6	34.846
14...20	35	10	40	25	90	1	10	55.77	6	44.846
20...28	45	15	60	40	100	1	15	83.66	8	64.536

Table 1: The standard tool sizes of the tool [1]

The required tool dimensions were selected from table 1 based on the calculated maximum radial depth, g_{max} = 7.5 mm, which falls under the g = 4...6 category. These dimensions ensure that the tool has sufficient strength and is compatible with the lathe clamping system.

In Figure 29, the tool rake angle (γ_{xu}) and the tool clearance angle (α_{xu}) of a flat form tool are depicted. The rake angle is the angle between the face of the cutting tool (where the chip flows off) and a line perpendicular to the cutting direction. The clearance angle is the angle between the flank of the tool (below the cutting edge) and the surface of the workpiece.

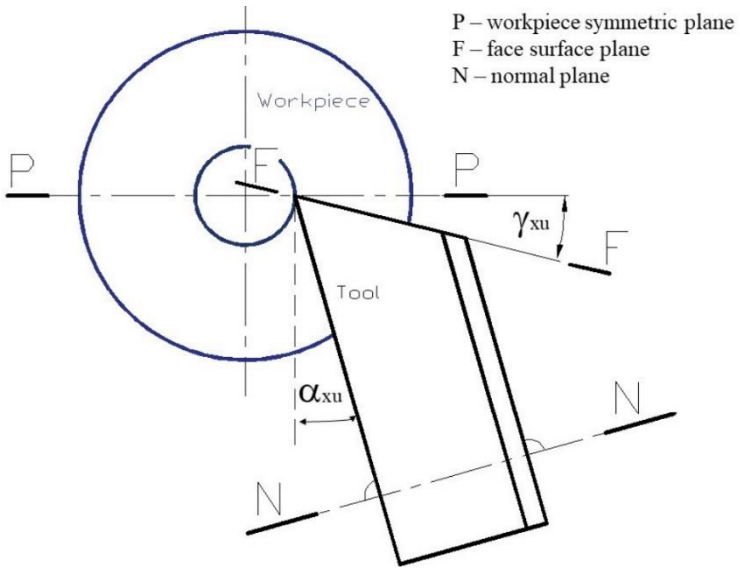

Figure 29: Depiction of tool rake angle and tool clearance angle [26]

The recommended values for the tool rake (γ_{xu}) and clearance (α_{xu}) angles based on the material type, ultimate strength, and hardness of the workpiece can be found in Table 2.

Material quality	Property		γ_{xu} [°]	α_{xu} [°]
	Ultimate strength [MN/m^2]	Hardness [HB]		
Steel	until 50	until 150	25	8…15
	50…80	150…235	20…25	
	80…100	235…290	12…20	
	100…120	290…350	8…12	
Cast iron		until 150	15	
		150…200	12	
		200…250	8	
Bronze and brass			0…5	
Copper and aluminium			20…25	

Table 2: Recommended values for tool rake (γ_{xv}) and clearance (α_{xv}) angles [1]

For the intended application in this paper, we selected steel as the workpiece material due to its high strength, wear resistance, and suitability for flat form tool application. The ultimate strength and hardness were considered as 50 MN/m^2 and 150[HB] respectively. The corresponding tool rake (γ_{xu}) and clearance (α_{xu}) angles were selected as 20° and 8° respectively.

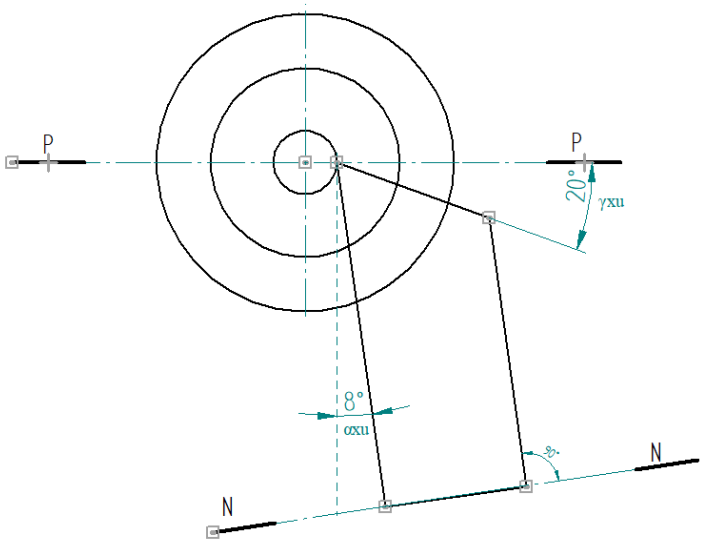

Figure 30: Interpretation of rake and clearance angles according to the selected values

With the changing of the cutting depth, the tool rake angle and the tool clearance angle also changes. These two angles are changing inversely as the cutting depth is changing. From the lowest diameter to the highest diameter, $\alpha_{x1} < \alpha_{x2} < \alpha_{x3}$ but $\gamma_{x1} > \gamma_{x2} > \gamma_{x3}$. This relationship can be seen in Figure 31. However, the sum of these two angles which is equal to the construction tool rake will always stay the same for every cutting point to preserve the cutting geometry [1].

The following is the equation to find the construction tool rake:

$$\gamma_{xv} = \gamma_{xu} + \alpha_{xu} \qquad (2)$$

In our case, the value of the construction tool rake was $\gamma_{xv} = 20° + 8° = 28°$. These angles are typically selected to be larger when using radial form tools, due to the difficulties faced during final operations, the need to reduce cutting force, and the fact that such tools are generally operated at low feed rates.

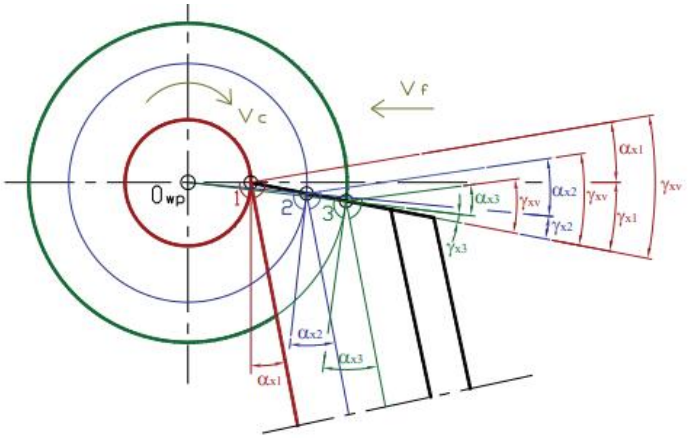

Figure 31: Geometric parameters of a forming tool relative to the workpiece [26]

2.2 Mathematical calculation of the form tool profile

To start off, we assigned a coordinate pair (r, l) to each profile point. Then we defined the radii r_1, r_2, r_3,…, r_{10} and the lengths l_1=0, l_2, l_3,…..,l_{10} for each of the 10 points labelled 1 through 10. The point with the smallest radius (point 1) was considered to be the reference point for the cutting tool's profile. Several points must be specified in case of arcs to ensure the tool profile's precision. All the 10 coordinate pairs can be seen in Figure 32. Finally, using point 1 as the starting reference and considering the rake angle(γ_{xu}) as 20° and the clearance (α_{xu}) angle as 8°, the tool's outline was drawn.

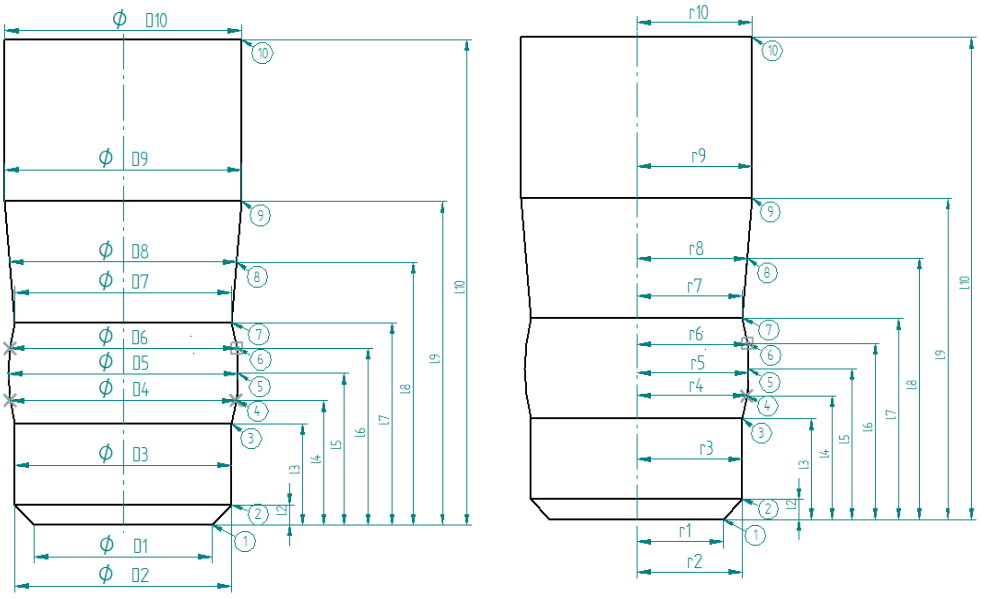

Figure 32: Determination of coordinate pair (r, l)

By establishing the first reference point and knowing the angles γ_{xu} and α_{xu}, the outline of the tool can be constructed. For the first profile point (in triangle formed by O_{wp}, K and point 1) in Figure 33, the equations are:

$$H_p = r_1 \cdot sin\gamma_{xu} \quad (3)$$

$$E_1 = r_1 \cdot cos\gamma_{xu} \quad (4)$$

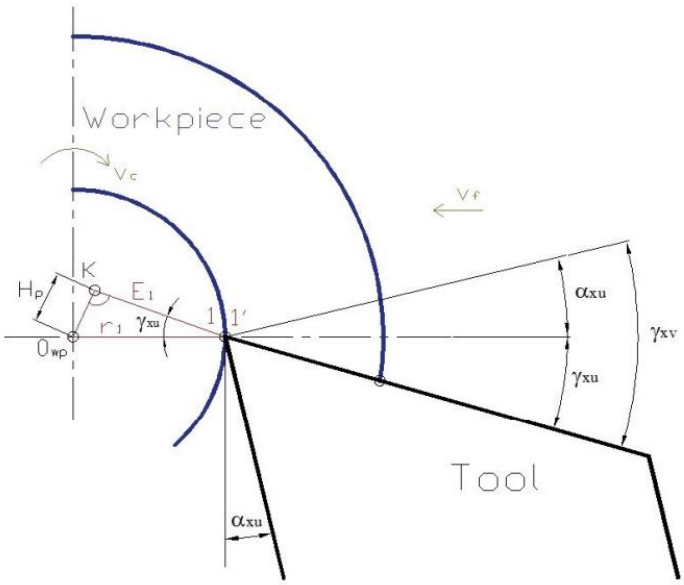

Figure 33: Alignment of the tool and the workpiece [26]

Incorporating our value of tool rake angle (γ_{xu}) and the value of r_1 from Figure 34 in the equations, we get $H_p = 7.695$ mm and $E_1 = 21.143$ mm.

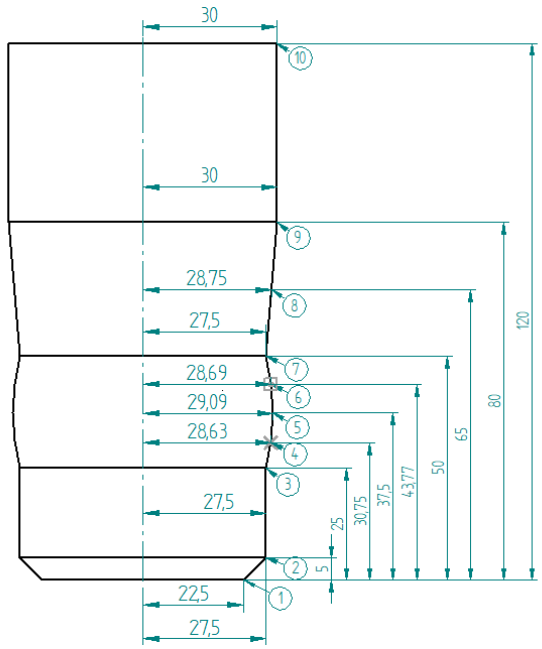

Figure 34: The r-l parameters on the workpiece

The value of Hp and the tool rake angles γ_{xu} ,γ_{x1} ,γ_{x2} , γ_{x3} at different workpiece points are essential for determining the dimensions E and F which are shown in Figure 35.

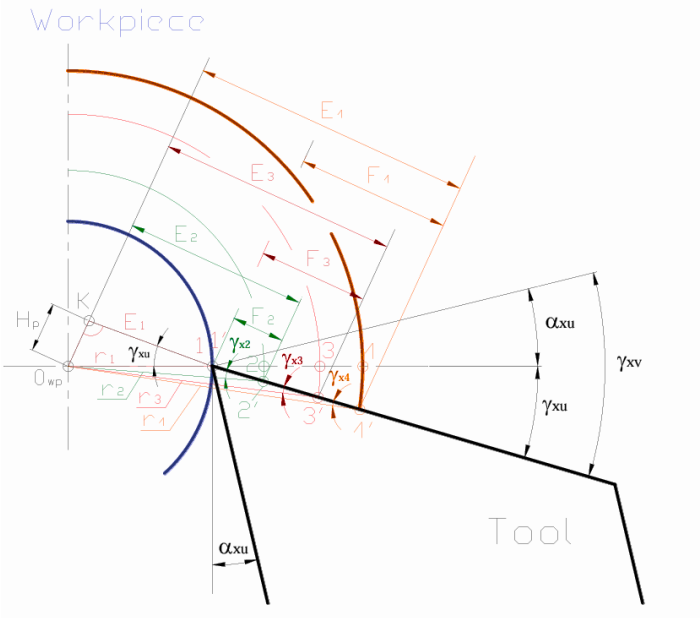

Figure 35: Determination of E and F sizes [1]

The equations for the second profile point (triangle formed by $O_{wp,}$ K and point 2):

$$sin\gamma_{x2} = \frac{H_p}{r_2} \quad (5)$$

$$E_2 = r_2 \cdot cos\gamma_{x2} \quad (6)$$

$$F_2 = E_2 - E_1 \quad (7)$$

- The equations of point 3 ($O_{wp,}$ K and point 3):

$$sin\gamma_{x3} = \frac{H_p}{r_3} \quad (8)$$

$$E_3 = r_3 \cdot cos\gamma_{x3} \quad (9)$$

$$F_3 = E_3 - E_1 \quad (10)$$

- The general equations for any arbitary point i on the workpiece are:

$$sin\gamma_{xi} = \frac{H_p}{r_i} \quad (11)$$

$$E_i = r_i \cdot cos\gamma_{xi} \quad (12)$$

$$F_i = E_i - E_1 \quad (13)$$

The values G_1, G_2, G_3,…..G_{10}, which define the outline curve of the tool, can be derived from the triangle constructions formed between points such as 1-2-2', 1-3-3', 1-4-4',…..1-10-10' on the N-N plane. This plane is oriented perpendicular to the flank of the tool. Each of these constructions forms a right-angled triangle. Figure 36 shows the dimensions of the G sizes. Using the known values of F and the construction tool, $\gamma_{xv} = \gamma_{xu} + \alpha_{xu}$ in the normal plane, the corresponding G values were calculated using the following expressions:

$$G_1 = 0 \quad (14)$$

$$G_2 = F_2 \cdot cos\gamma_{xv} \quad (15)$$

$$G_3 = F_3 \cdot cos\gamma_{xv} \quad (16)$$

$$G_i = F_i \cdot cos\gamma_{xv} \quad (17)$$

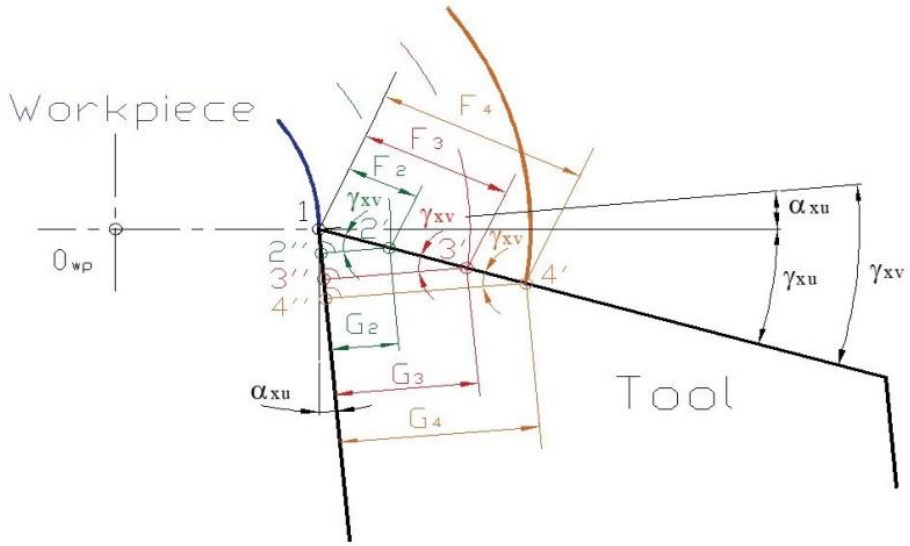

Figure 36: Establishment of G sizes [26]

The calculation result of the workpiece profile was then illustrated through the tabulated data of tool profile parameters, and the corresponding plot of G sizes against tool length. These outputs collectively define the geometry of the cutting tool required to generate the specified contour of the workpiece.

i	r (mm)	l (mm)	γxi (°)	γxi (radian)	E (mm)	F (mm)	G (mm)
1	22.5	0	20.01232182	0.349280907	21.14142852	0	0
2	27.5	5	16.26020471	0.283794109	26.4	5.258571477	4.643043027
3	27.5	25	16.26020471	0.283794109	26.4	5.258571477	4.643043027
4	28.63	30.75	15.6017153	0.272301301	27.57511378	6.433685257	5.680606911
5	29.09	37.5	15.34887629	0.267888428	28.05241701	6.910988485	6.102040647
6	28.69	43.77	15.56825873	0.271717374	27.637404	6.495975479	5.735605913
7	27.5	50	16.26020471	0.283794109	26.4	5.258571477	4.643043027
8	28.75	65	15.53494722	0.271135978	27.69968411	6.558255591	5.790595987
9	30	80	14.87236545	0.259571745	28.99499957	7.853571046	6.93429165
10	30	120	14.87236545	0.259571745	28.99499957	7.853571046	6.93429165

Table 3: The calculated geometric parameters

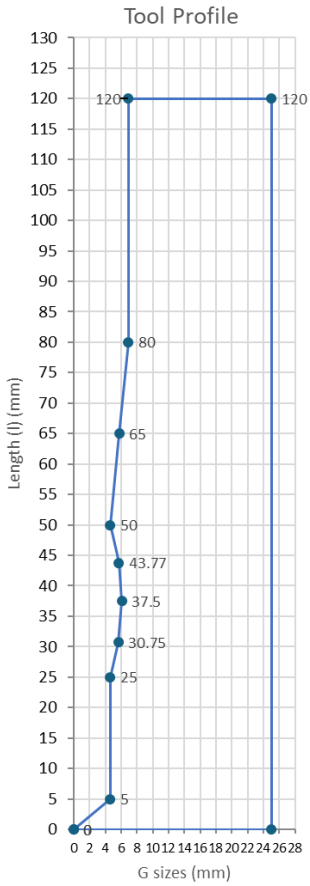

Figure 37: Representation of tool profile on the G-l Descartes coordinate system

3 Constructional Evaluation of Design Correctness

3.1 Geometrical Construction of the Tool

The outline views of the workpiece and the tool are located on different planes. The P plane represents the symmetrical plane of the workpiece, where its contour is defined. The F plane corresponds to the face surface of the tool, and the N plane is the tool's normal plane- this is the plane used for defining the tool profile.

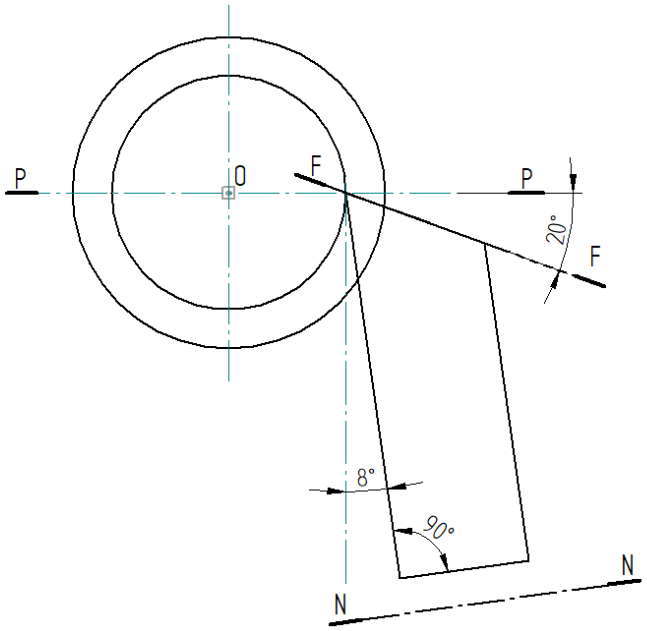

Figure 38: The position of the planes

The dimensions of the tool were acquired from the standard sizes of the tool from Table 1. Once the tool and the workpiece were properly aligned as shown in Figure 38, created using the CAD software, Solid Edge Draft, the following steps were followed to verify the correctness of the design. Throughout the whole process, two key projections were used- one onto the P plane (symmetry plane) and the other onto the N plane (the normal plane).

1. **Define the Workpiece Geometry:** Identified and marked the corner points of the workpiece as 1,2,3,4,……10. Since the workpiece includes an arc, considering additional intermediary points improves the accuracy of the resulting arc projection onto the tool's normal plane. Refer to Figure 34 for defining the workpiece geometry.

2. **Front view to top view projection on P-plane:** Once the points were identified on the front view of the workpiece, these were projected onto the top view on the symmetrical plane P. A close-up view of the projections are shown in Figure 40.

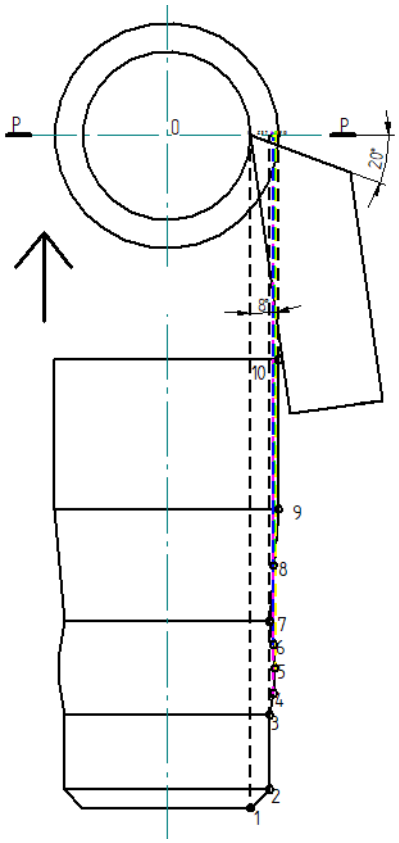

Figure 39: Projections onto the top view

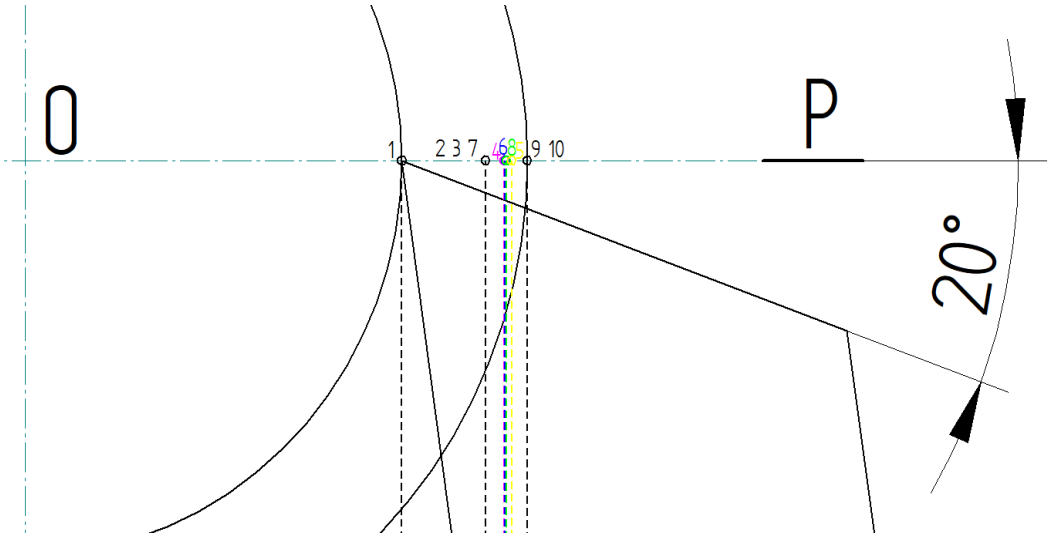

Figure 40: Close-up view of the projections onto the top view

3. **Compute radii:** The radii are calculated as the distance between the centre point and the points 2,3, 4,……9.

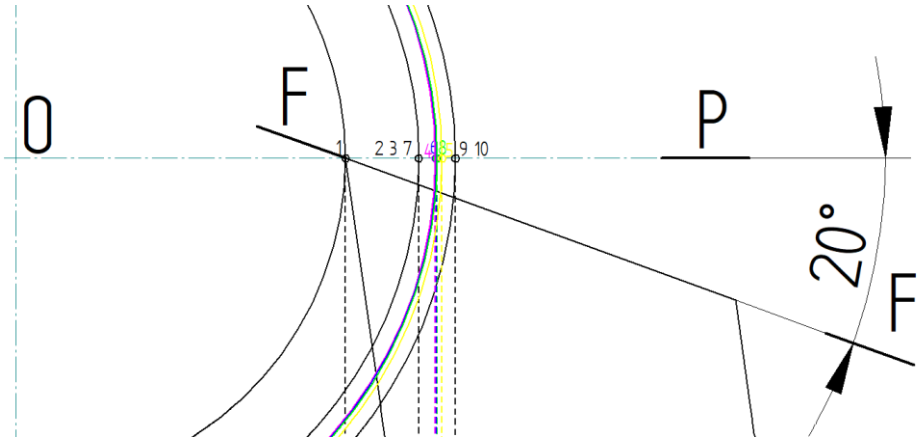

Figure 41: Depiction of the radii

4. **Circular reference and intersection at the flank surface:** Using the previously found radii, circles were drawn from the center of the workpiece as shown in Figure 41. This circle intersected the tool's face surface at points 2', 3', 4',…..10'. These points lie on the F plane, which is the face surface plane of the tool as shown in Figure 42.

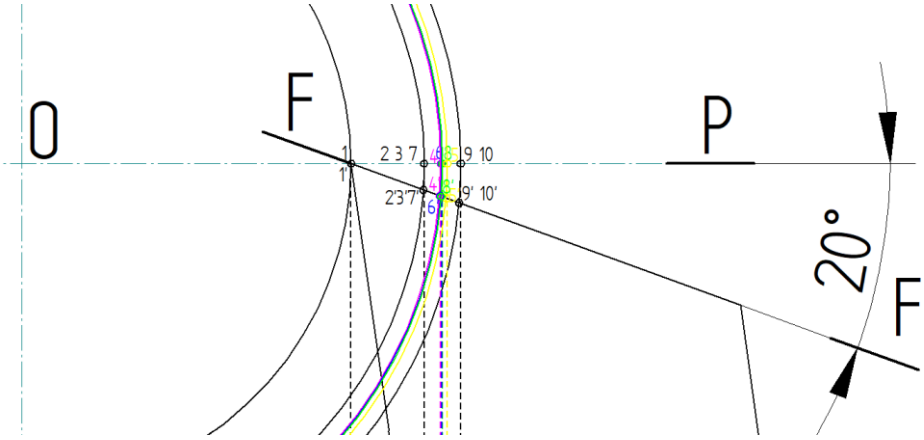

Figure 42: Intersection at the face surface

6. **Symmetry Consideration:** Since the tool aligned with the P plane of the workpiece, points 1 and 1' coincided.
7. **Projection onto normal plane:** The points 1', 2',3',4',…10' were then projected onto the tool's normal plane along the flank surface.
8. **Determination of final tool point:** The intersection of these projection lines with the height levels l_2, l_3, l_4,…….l_{10} gave the points, 2", 3", 4",….10" on the tool's normal plane. Point 1" was defined as the

projection of the tool point onto the normal plane, where the vertical height is zero.

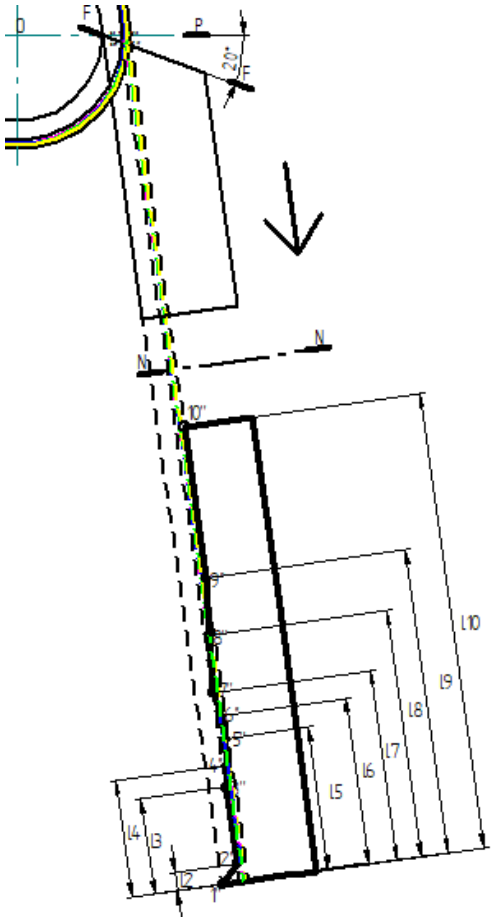

Figure 43: Projection on normal plane to get the final tool profile

By completing the projection steps for all the necessary points, the tool profile is fully established. This final profile ensures the tool replicates the contour of the workpiece as intended.A clear illustration of the tool profile is shown in Figure 44.

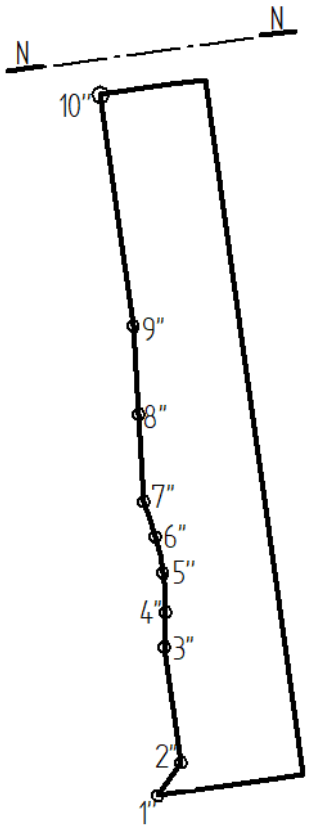

Figure 44: Clear depiction of the tool profile

Both the P plane and N plane projection processes are illustrated in detail in Figure 45. This figure provides a step-by-step representation of how to get the final tool profile by construction, starting from projection on to the P plane and then onto the N plane.

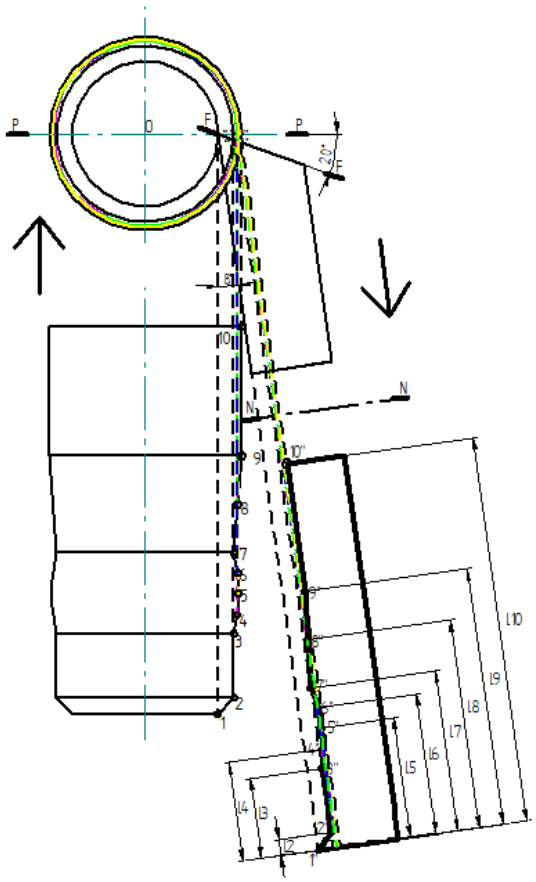

Figure 45: P plane and N plane projections

Although the form tool design in Figure 44 is geometrically accurate, some practical concerns have appeared regarding its load simulations. Specifically, the following are the mechanical limitations that arose due to the slenderness of the tool's external structure:

- Insufficient structural rigidity under cutting loads
- High deflection and the likelihood of vibration-induced instability during machining
- Risk of tool breakage or uneven wear due to inadequate cross-sectional mass

To mitigate these issues, a redesign is being proposed in Figure 46 featuring a thicker tool body while preserving the functional profile that interacts with the workpiece. Previously, the form tool was selected based on the standard dimensions corresponding to the range = 6….10 in Table 1. The associated tool dimensions were:

- A = 19, B = 6, C=25, D=15, V=75, r=0.5

However, to address load capacity and structural rigidity issues, the tool was needed to be upgraded to a larger standard size. This new set of dimensions fell under the g = 14….20 category in Table 1.

- A =35, B=10, C=40, D=25, V=90, r=1

Figure 46: Externally modified tool profile

The jump from A=19 to A=35 and B=6 to B=10 almost doubles the width, significantly increasing its cross-sectional area and stiffness. Moreover, better support across the tool shank is also ensured by the larger value of C=40 instead of C=25. Overall, the follwoing are the benefits that could be gained due to the modifications of the tool geometry:

- Reduced deflection.
- Risk of chatter minimised during cutting operations.
- Increased thermal capacity and reduced localized overheating.

Both the modified P and N plane projections are shown in Figure 47.

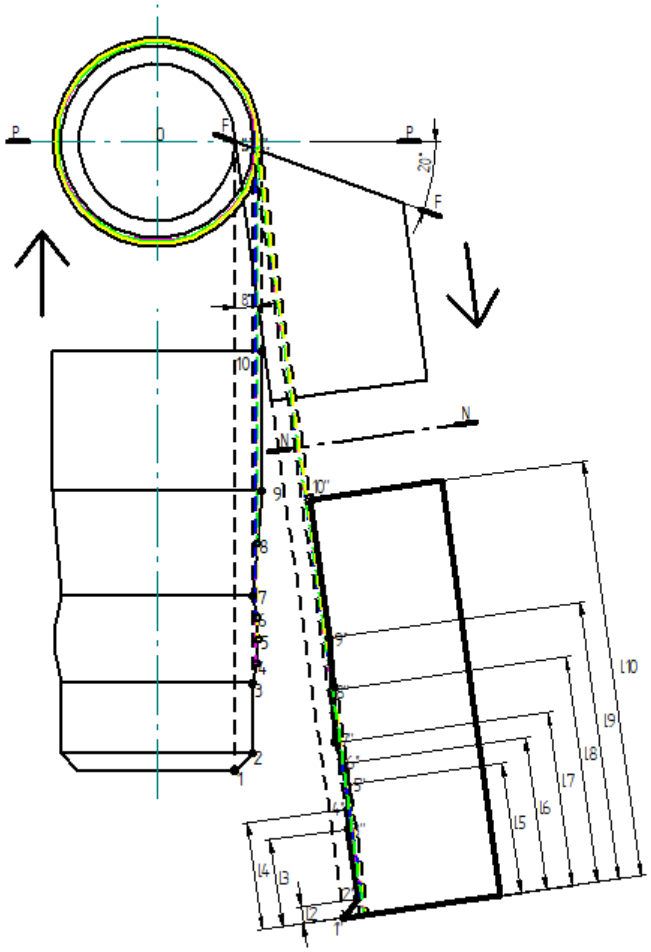

Figure 47: Modified P and N plane projections

The required clamping mechanism must now accommodate larger diameters (d_{r1}=10, d_{r2}=6) and deeper thread engagement (M_1=55.77, M_2=44.846). Tool holders or fixtures must be adapted accordingly.

In conclusion, the new form tool design resolves critical capacity limitations due to the thicker and more robust external geometry. This adjustment ensures mechanical durability, dimensional accuracy, and operational safety, without compromising the cutting profile essential for shaping the workpiece.

3.2 CAD Model of the Tool

From the defined geometry of the workpiece and the modified geometry of the tool, CAD models were created using Solid Edge. Referring to Figure 27, the chamfered section of the tool was increased as well as the straight section was introduced, which can be seen on Figure 48 and 49.

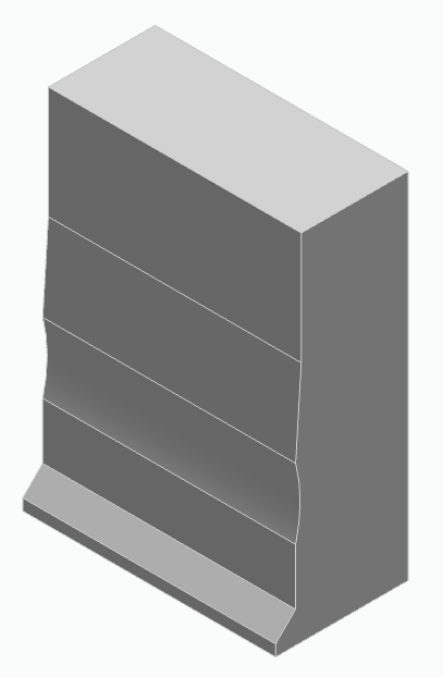

Figure 48: CAD model of the tool

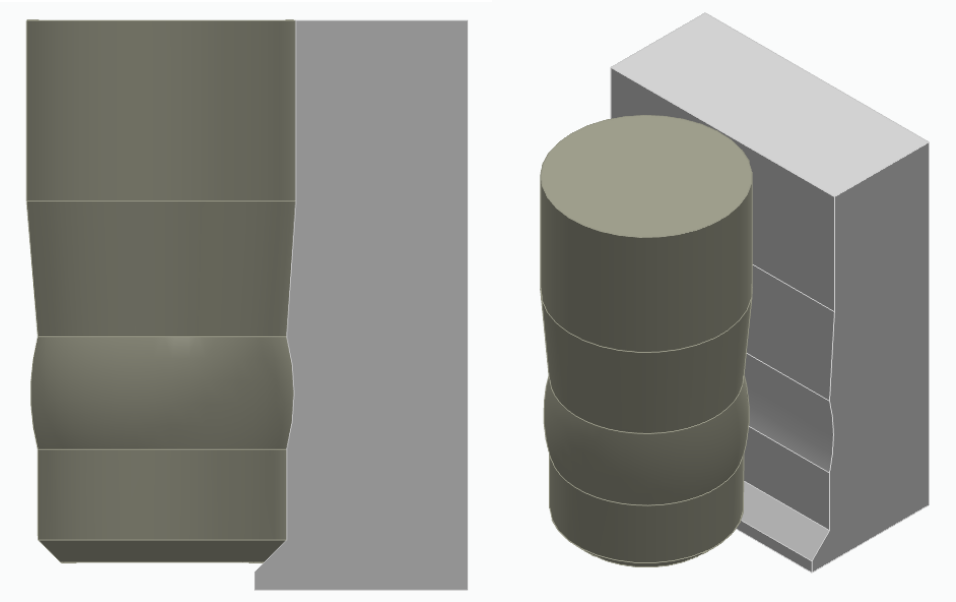

a *b*

Figure 49: The assembly of the tool and the workpiece where a) Front view b) Isometric view

4 Design and Optimization of the Tool Clamping Device and Its Manufacturing Process

The clamping device developed in this work is based on the principle of single-position tool post. The primary purpose of the device is to rigidly secure the tool in position on the machine cross-slide while ensuring sufficient strength and repeatability during machining operations.

The CAD model of the clamping device (Figure 50) was designed to accommodate the dimensions of the flat form tool developed in this thesis.

While the geometry of the clamping device was scaled to fit our wider form tool, the fundamental architecture and the functions of its components remain unchanged. These include:

- **Tool Post:** This is the central clamping structure of the system. The tool post serves as an intermediary between the tool holder and the cross-slide. It generally provides a rigid platform to transmist significant cutting forces. A T-nut is also engaged with the machine's T-slot to secure the tool post to the cross-slide.
- **Tool Holder:** The tool holder serves as the clamping body that directly installs the flat form tool. Four socket head cap screws apply the clamping force by pressing the tool firmly against the. To facilitate positioning and manual height adjustment, a knurled thumb wheel was included into the design as well.
- **T-Nut:** The T-nut is installed on the T-slot of the cross-slide, providing a rigid base for claping. It also prevents rotations of the clamping body.
- **Socket Head Cap Screws:** These heavy-duty screws provide the required clamping force against the surface of the holder to secure the tool in place. Their socket design allows for high torque transmission while remaining compact.
- **Knurled Thumb Wheel:** The knurled thumb wheel enables manual adjustments during setup, improving operator ergonomics.
- **Studs, Hex Nuts and Washer:** The studs act as the primary anchor. The hex nuts secure the studs in position, while the washer distributes the clamping load evenly.

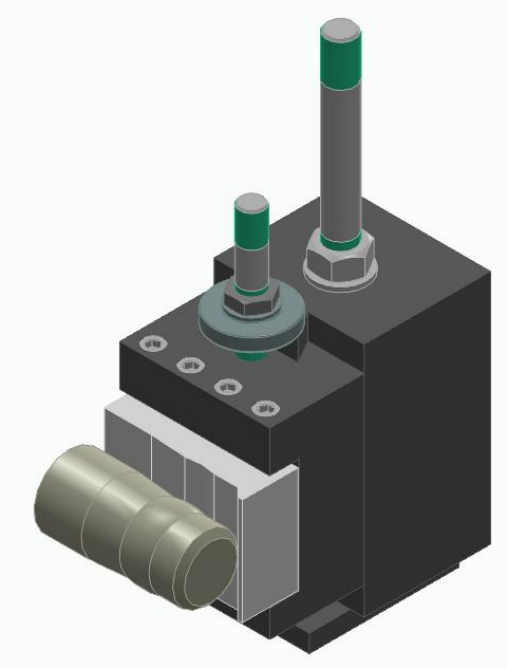

a

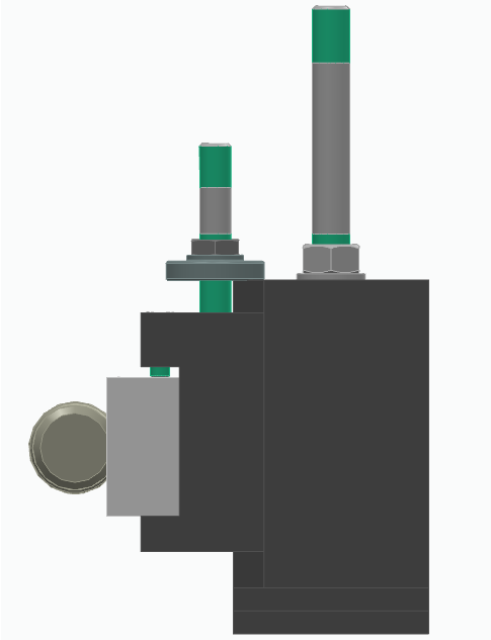

b

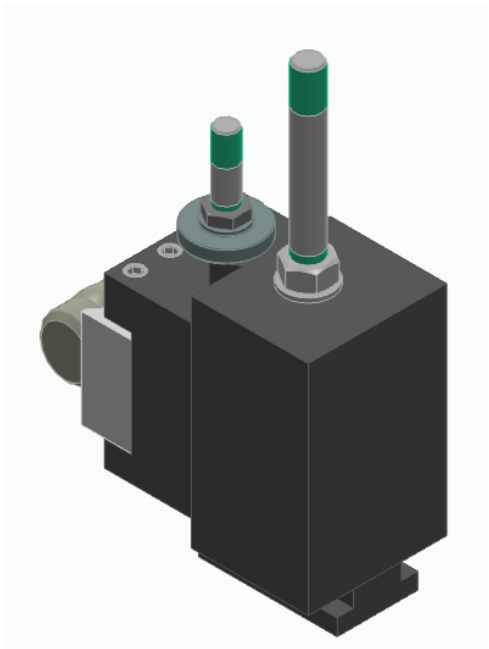

c

Figure 50: Different views of the flat form tool and its clamping device assembly

To validate the applicability of the designed clamping system, a production-scale lathe is recommended. The Kingston HR2000 engine lathe, with swing

capacity of 30", provides sufficient rigidity and power to accommodate heavy duty tooling.

For the tool post, a custom design was developed. However, its geometry was partly derived from the Aloris DA-series specifications. In particular, the base dimensions were adapted to accommodate the T-nut, ensuring industry-standard to remain mechanically compatible with the HR2000's cross-slide T-slot arrangement.

Since T-slot dimensions are machine-specific and not publicly documented for the HR-2000, the T-nut in the CAD assembly was modeled as a reference. In practice, it would be supplied as blank and then machining would be done to match the measured slot dimensions of the HR2000 compound slide. This ensures that the custom-designed post can be securely mounted to the machine while acknowledging the need for final machining adjustments during implementation.

To support the CAD design and functional description, technical drawings were prepared for the tool post, tool holder and the complete clamping assembly. These drawings defined the dimensions and geometry necessary for manufacturing and inspection.

Figure 51 shows the techncial drawing of the tool holder, which serves as the clamping body for the 120 mm long major cutting-edge form tool. The drawing highlights the major dimensions which are required to manufacture the tool holder accuartely. The clamping screw locations are also shown where four M12 socket head screws were employed to firmly clamp the tool against the holder's surface.

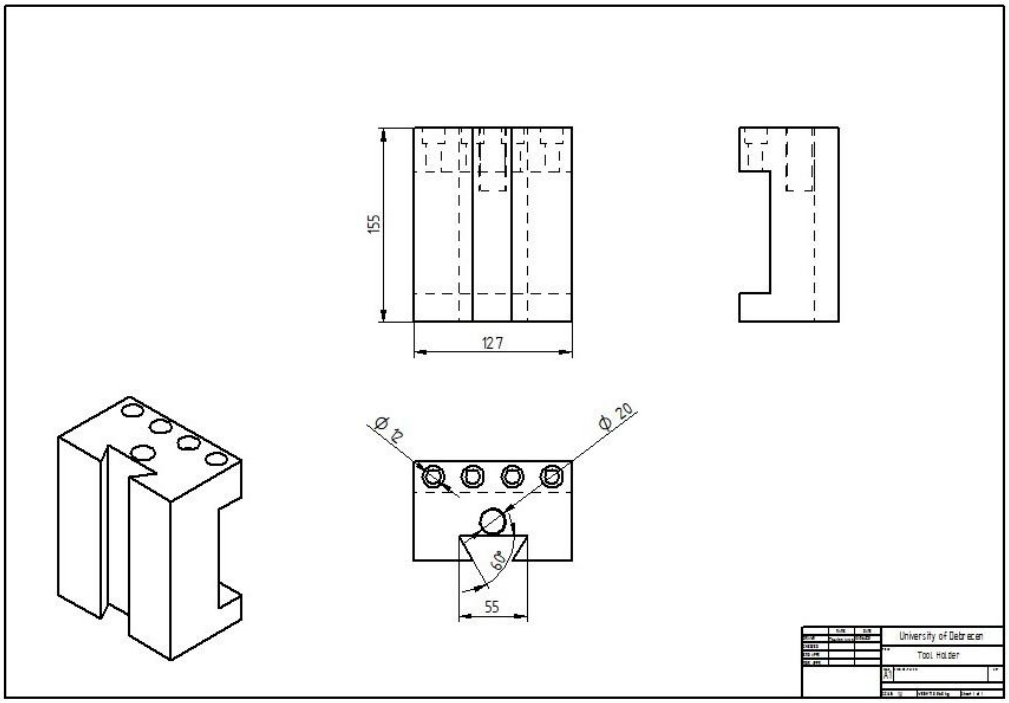

Figure 51: Technical drawing of the tool holder

The technical drawing of the tool post is shown in Figure 52. The key dimensions are provided for machinability and alignment with the HR2000 cross-slide T-slot. The geometry, partly taken from Aloris DA-series specifications, was adapted to accommodate the T-nut and the stud in the T slot. A M24 stud with matching hexagon nut and washer was used to connect the tool post and T-nut, ensuring a secure and rigid attachment.

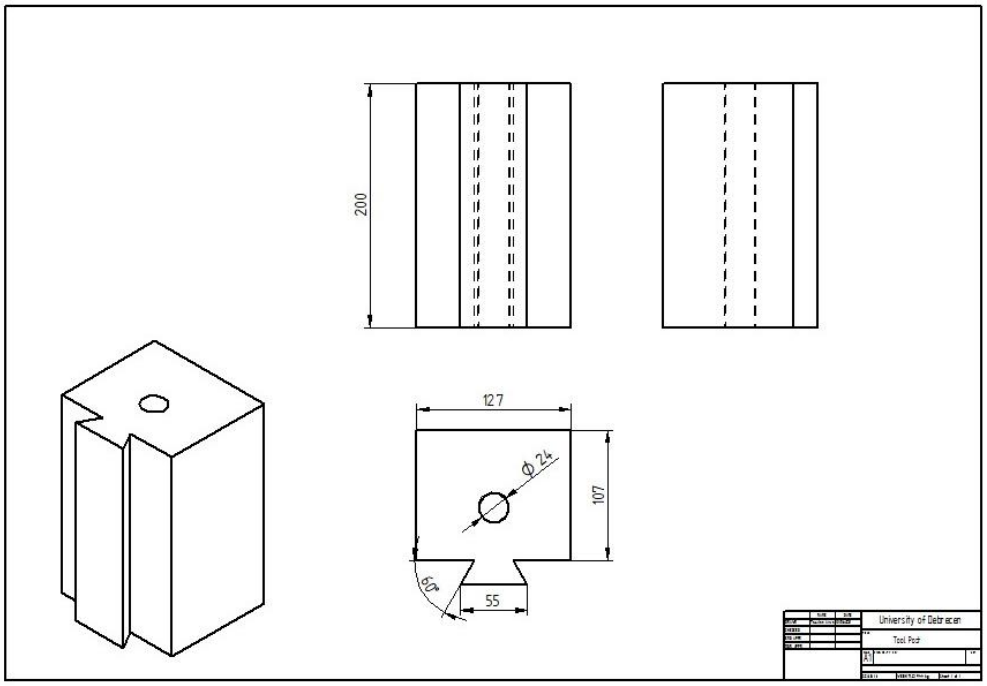

Figure 52: Technical drawing of the tool post

The full assembly drawing, combining the tool post, tool holder, fasteners and T-nut is shown in Figure 53. This drawing was created to highlight the overall configuration of the clamping system. It further shows how the individual components are integrated into a single functional assembly. The drawing also includes a Bill of Materials (BOM), listing each component used to construct the clamping device.

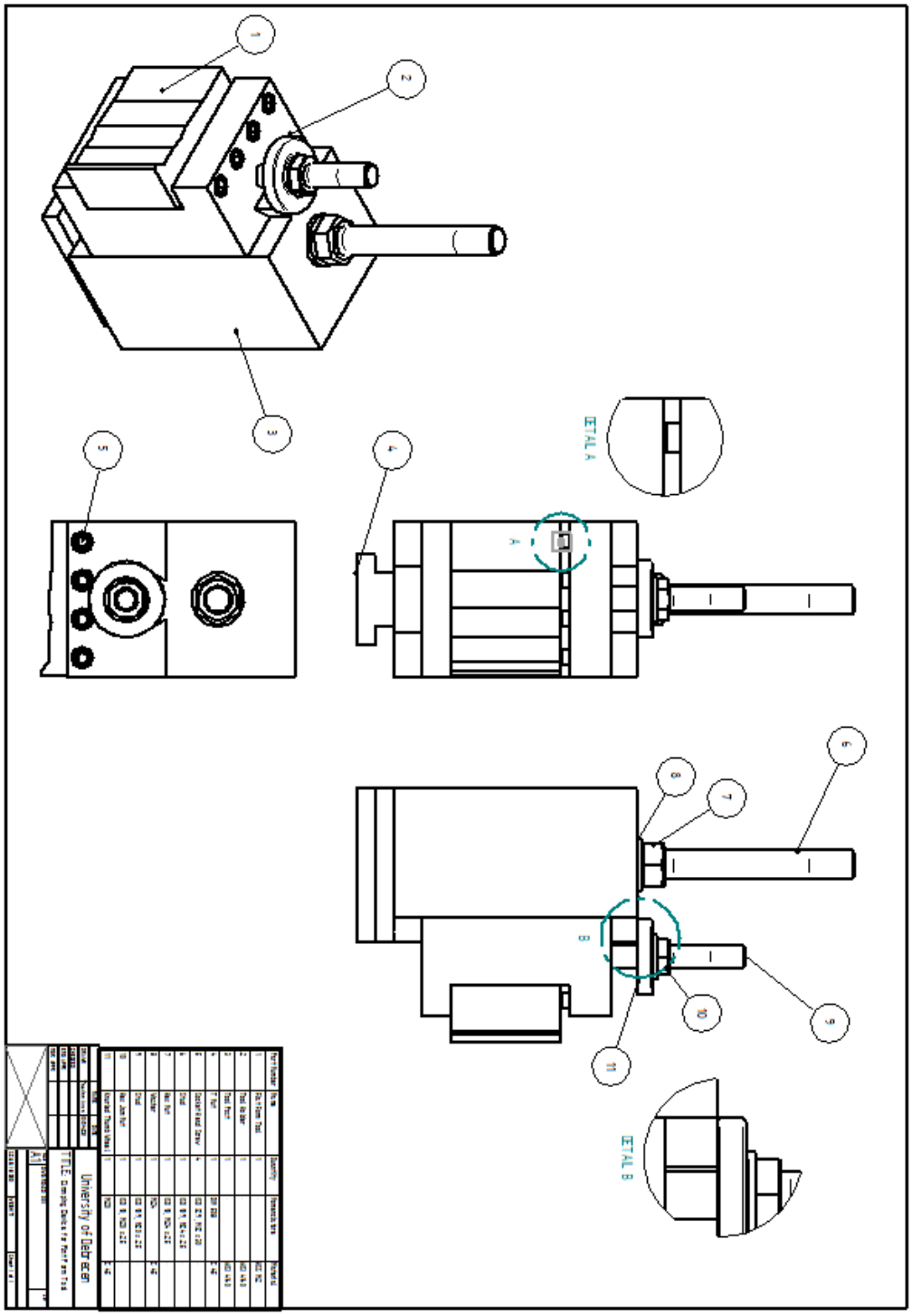

Figure 53: Assembly drawing of the clamping device

A complete bill of materials (BOM) was made to classify all the components required for the clamping device. It consists of both standard components (such as studs, nuts, washers, and socket head cap screws) and custom-designed parts (tool post, tool holder and T-nut). Part number, designation, quantity, and material specification are listed for all items, ensuring traceability during fabrication and assembly.

Part Number	Name	Quantity	Nomenclature	Material
1	Flat Form Tool	1	-	HSS M2
2	Tool Holder	1	-	AISI 4140
3	Tool Post	1	-	AISI 4140
4	T Nut	1	DIN 508	C-45
5	Socket Head Screw	4	ISO 12.9, M12 x 30	-
6	Stud	1	ISO 10.9, M24 x 2.5	-
7	Hex Nut	1	ISO 10, M24 x 2.5	-
8	Washer	1	M24	C-45
9	Stud	1	ISO 10.9, M20 x 2.5	-
10	Hex Jam Nut	1	ISO 10, M20 x 2.5	-
11	Knurled Thumb Wheel	1	M20	C-45

Table 4: Bill of Materials of the clamping device

The design and documentation of the clamping device gave a complete solution tailored for the 120 mm flat form tool. By combining standard components with custom-made parts, both strength and adaptability were achieved in the assembly. Paired with the technical drawings, the BOM provides a clear pathway from concept of the flat form tool to successful fabrication. This ensures that the proposed device is both theoretically sound and practical for implementation.

5 Determination of the technological parameters and performing finite element analysis.

5.1 Determining key process parameters

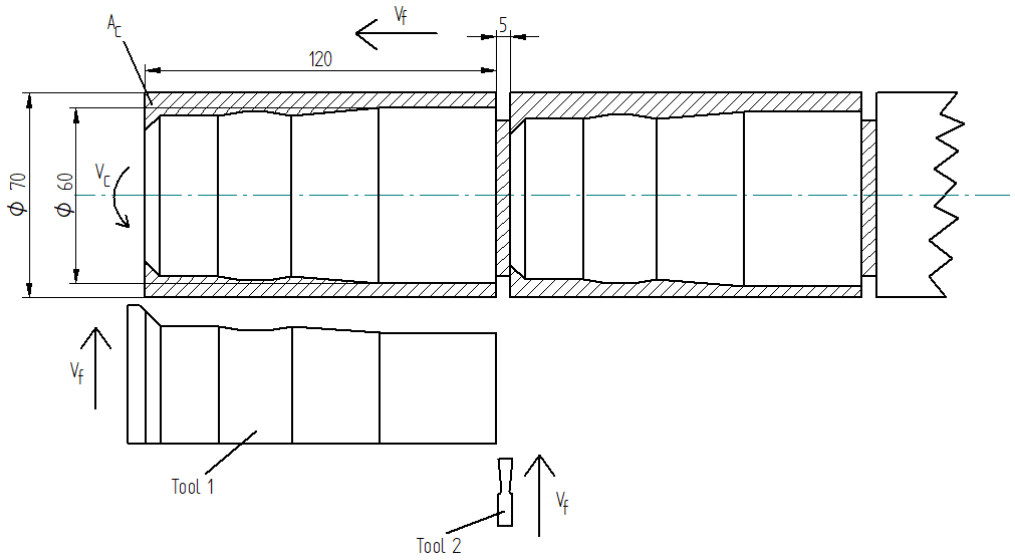

Figure 54: Workpiece blank with finished diameter, showing tool kinematics

For machining the part shown in Figure 54, the maximum finished diameter of the workpiece is 60 mm. Therefore, to ensure adequate material allowance for turning operations, a cylindrical blank material of 70 mm diameter was selected. Since the part would be manufactured in serial production, a parting tool was incorporated with a width of 5 mm to separate each finished piece from the blank.

V_c represents the tangential cutting speed due to workpiece rotation. The feed velocity is represented as V_f, indicating the relative linear movement of the form tool into the rotating workpiece. The chip cross-sectional area, A_c is the area of the material engaged by the tool before being deformed into a chip. It serves as a key factor in determining cutting forces.

To evaluate the cutting forces, the chip cross sectional area, A_c, must first be determined. It serves as the basis for subsequent cutting force and power calculations. As seen on Figure 55, the total area to be removed is 1497.09 mm^2, which corresponds to 748.55 mm^2 per side.

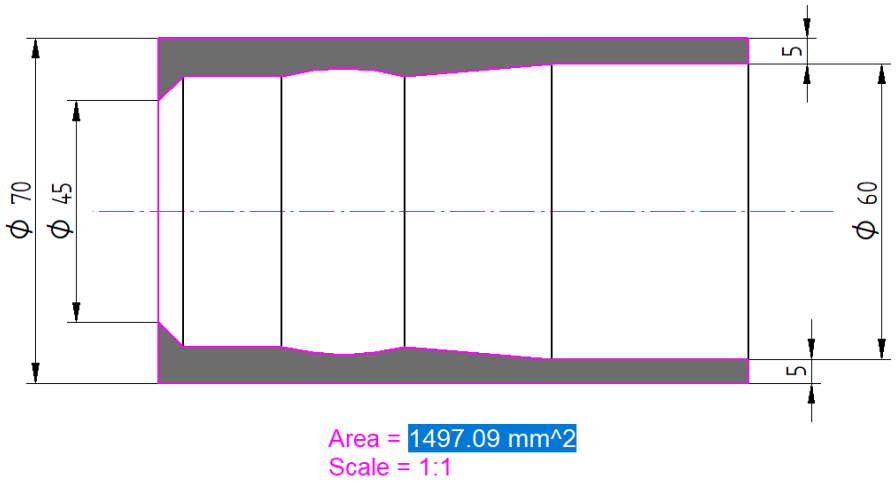

Figure 55: Determination of stock area to be removed

To find A_c, we should also determine the feed rate. Let's consider the feed rate to be 0.10 mm/revolution as it falls within the acceptable range [27]. This means in every revolution of the workpiece, the tool advances 0.10 mm radially into the stock.

The maximum radial plunge of the tool is determined by the difference between the initial diameter of the stock and the final smallest diameter of the workpiece i.e. 70 mm – 45 mm = 25 mm. This makes 12.5 mm maximum plunge per side.

Thus, the total number of revolutions required to achieve the final workpiece profile is:

$$\frac{Distance\ of\ plunge}{Feed\ rate} = No.of\ rev \qquad (18)$$

$$\frac{12.5\ mm}{0.10/mm} = 125\ revolutions$$

Consequently, with the following formula, we can find the chip cross-sectional area, A_c :

$$\frac{Area\ removed\ on\ one\ side}{No.of\ rev} = A_c \qquad (19)$$

$$\frac{748.55\ mm^2}{125\ revoltions} = 5.99\ mm^2$$

Now, the following formula can be used to find out the cutting force, F_c.

$$F_c = k_c \times A_c \qquad (20)$$

$$F_c = 2000 \frac{N}{mm^2} \times 5.99\, mm^2 = 11980\, N$$

In this expression, k_c denotes the specific cutting force, which is a material and tool depended constant. For steel, recommended value of k_c is within the range (1500 - 2500) N/mm^2 [28]. Therefore, using 2000 N/mm^2 as the value of specific cutting force, we get 11980 N cutting force.

The resulting force F_c provides the basis for subsequent calculations of the radial force, F_p and the feed force, F_f.

$$F_p = 0.3 \times F_c \quad (21)$$

$$F_p = 0.3 \times 11980 = 3594\, N$$

$$F_f = 0.3 \times F_c \quad (22)$$

$$F_f = 0.3 \times 11980 = 3594\, N$$

5.2 Finite Element Analysis of the Tool and the Clamping Device Assembly

To validate the structural integrity of the tool and the clamping device assembly under expected operating loads found previously, a static structural analysis was performed in ANSYS Workbench.

Since before performing the analysis, it is essential to define accurate material properties for both the tool and the clamping device, Table 5 shows the materials used and their corresponding properties.

Component	Material	Density	Young's Modulus	Poisson Ratio	Tensile Yield Strength	Compressive Yield Strength	Tensile Ultimate Strength	Compressive Ultimate Strength
Flat Form tool	HSS M2	8140 kg/m^2	210 GPa	0.29	2200 MPa	2600 MPa	3000 MPa	3100 MPa
Tool Holder	AISI 4140 steel	7850 kg/m^2	210 GPa	0.30	900 MPa	950 MPa	1100 MPa	1200 MPa
Socket Head Screws	Alloy steel	7850 kg/m^2	210 GPa	0.30	1080 MPa	1080 MPa	1220 MPa	1220 MPa

Table 5: Material Properties [29,30,31]

Once the materials were assigned to their respective components, the next step involved meshing the assembly geometry to prepare it for finite element analysis. Since the accuracy of the static structural analysis strongly depends on the quality and refinement of the mesh, a global element size of 2 mm was applied to the entire assembly to ensure a balance between computational efficiency and the

result accuracy. Furthermore, as the major cutting edge of the tool tends to experience higher stress concentrations, the mesh in this region was refined by a factor of three, resulting in an element size approximately one-third of the global mesh (~0.67 mm)

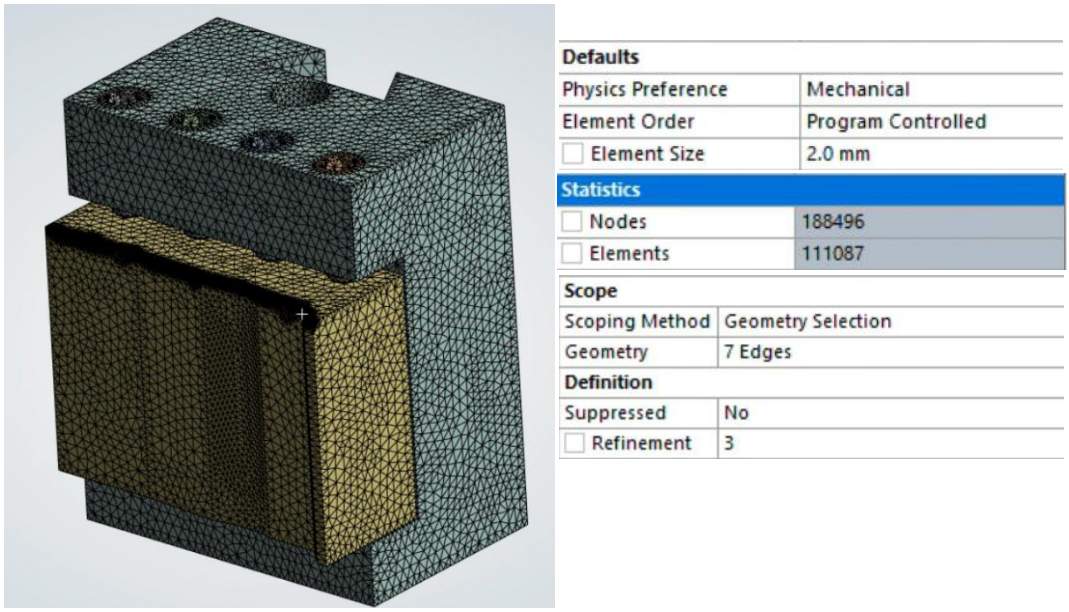

Figure 56: Meshed model with 2 mm global element size and 3x refinement at the cutting edge

Following meshing, an external cutting force of 13,014 N was given to the major cutting edge of the tool to replicate the real machining conditions. The force was defined in the Cartesian coordinate system, with Fx= 3595 N, Fy= -3594 N, and Fz= -11,980 N. The load was applied along the selected edges of the cutting region which would be in contact with the tool, as shown in Figure 57.

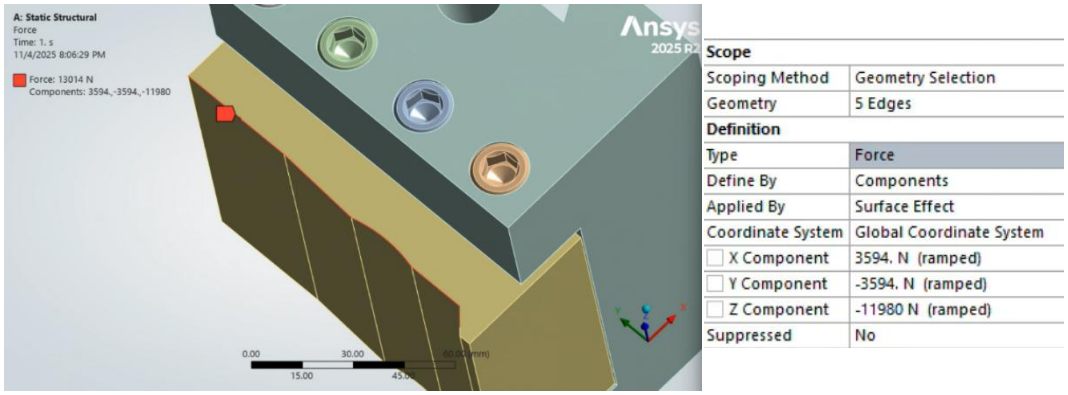

Figure 57: Forces applied along the major cutting edge

A fixed support was also applied to the bottom surface of the tool which rests on the tool holder. This was done to restrict all translational and rotational movement at the base, simulating real-world machining condition.

The first and the foremost analysis that was needed to be done was the equivalent (von Mises) stress distribution. This stress analysis determines the yielding possibility of a material under multi-axial stress. Figure 58 illustrates the equivalent (von Mises) stress distribution under the applied cutting load of 13,014 N. The maximum stress was observed to be 1318.5 MPa, concentrated near the major cutting edge of the tool. This region exhibits such high stress behaviour because of the sharp geometric changes. On the other hand, the minimum stress value was observed to be approximately 2.48 x 10^6 MPa, occurring at the lower part of the tool holder. This suggests a minimal loading in this area. It can also be obsereved that the stress gradient smoothly transitions from the cutting edge toward the clamping body. This is due to the signifying effective constraint at the base and appropriate load transfer.

When compared to the tensile yield strength of HSS M2 (2200 MPa), it can be concluded that the tool operates well within the safe limit with a factor of safety (FoS) of roughly 1.67. This confirms a structurally sound design of the tool under the given static loading conditions.

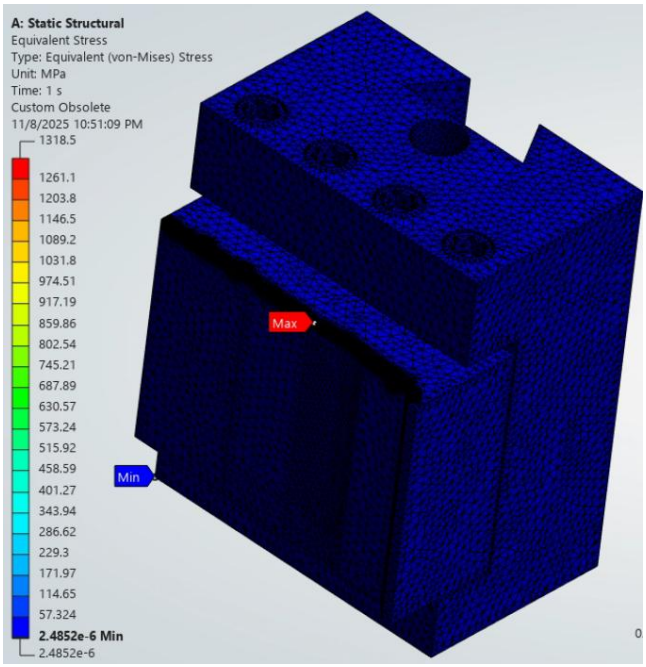

a

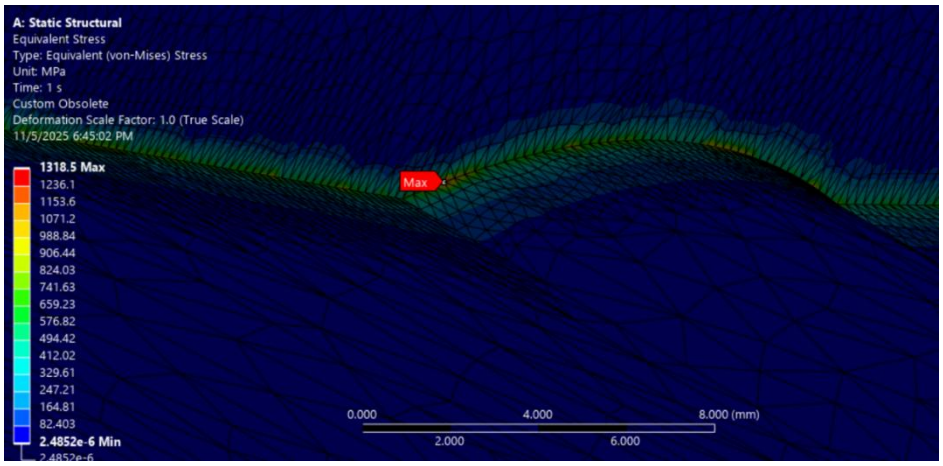

b

Figure 58: Equivalent (von Mises) Stress distribution

Additionally, the total deformation of the tool and clamping assembly was found to assess the overall stiffness of the system under the applied load. As shown in Figure 59, maximum deformation of 0.00686 mm was recorded near the major cutting edge, whereas the minimum deformation was found to be effectively 0 mm. This small magnitude of deformation demonstrates that the assembly has high structural rigidity and can withstand the applied force without any major deflection.

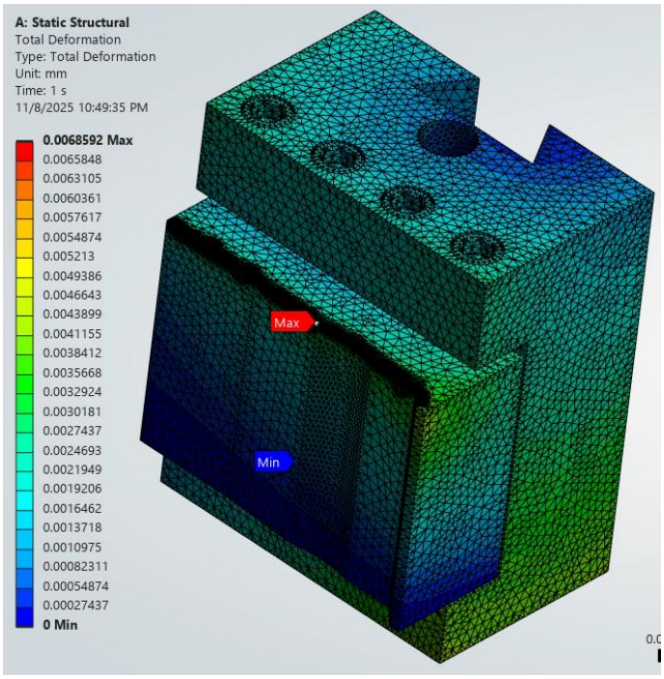

Figure 59: Total deformation of the tool and clamping assembly

Furthermore, to understand the elastic behavior of the assembly, the distribution of normal elastic strain along the X-axis was also assessed. The maximum strain observed was 0.001553 mm/mm, whereas the minimum strain value was -0.000375 mm/mm. Both maximum and minimum normal strains occur along the cutting edge. As expected of bending type deformation, one side of the edge experiences tensile strain, while the opposite side experiences compressive strain. The relatively small strain magnitude means that the material remains well within the elastic limit, with little to no plastic deformation under the static loading. We also found evidence of consistency as the strain pattern closely follows the stress and deformation distributions observed earlier.

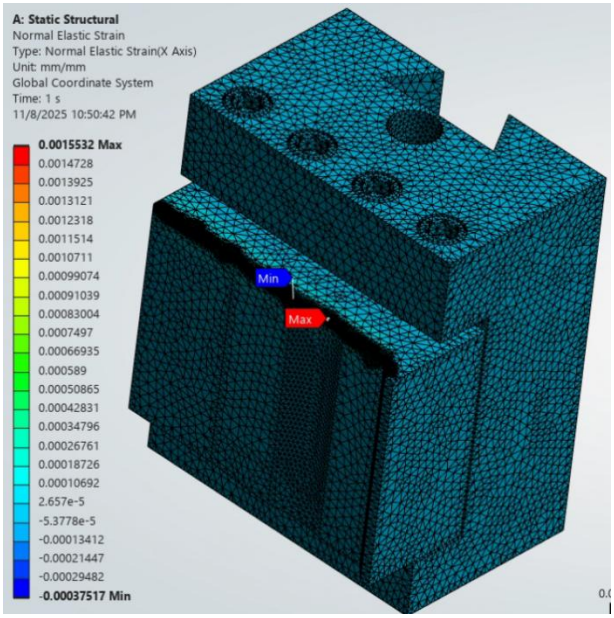

a

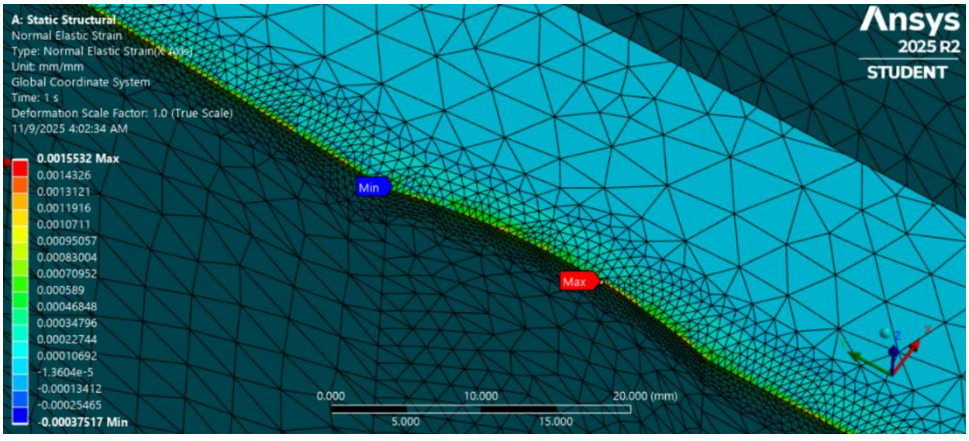

b

Figure 60: Normal Elastic Strain (X-axis) distribution

Finally, Figure 61 shows the normal stress distribution along the x-axis. It is used to examine the directional stress behaviour of the tool and clamping assembly. The maximum normal stress value reached 203.14 MPa, whereas the minimum value was -303.82 MPa. The presence of both tensile and compressive stress zones suggests a combination of bending and axial loading during operation. The magnitude of normal stress remains under the yield strength of HSS M2 (2200 MPa), confirming that the tool remains within the elastic range under static loading.

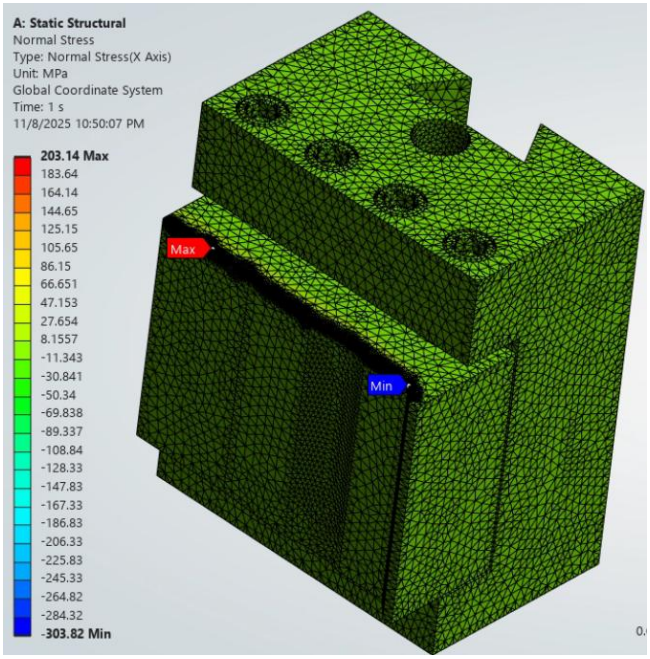

a

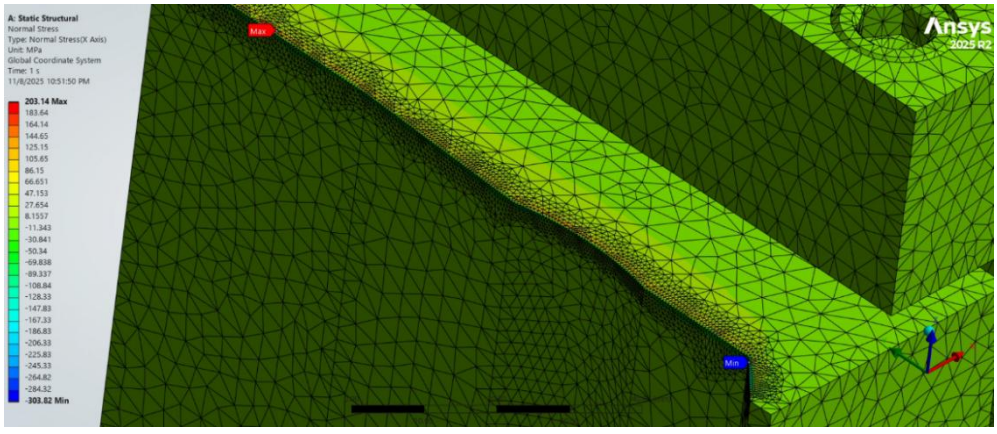

b

Figure 61: Normal Elastic Stress (X-axis) distribution

6 CONCLUSION

This study presented an analytical, contructional, and computational evaluation of a flat form tool and its clamping device assembly. Through mathematical calculations, the tool geometry was designed meticulously, ensuring accuracy and manufacturability. Following this, constructional verfication was carried out in Solid Edge Draft to further verify the geometry of the tool. Since during constructional evaluation, potential possibilties of structural limitations arose, modifications were made to the flat form tool to ensure structural integrity. As a result, the new tool dimensions were finalised within the g = 14 mm to 20 mm range. These new modifications made to the tool would ensure structural stability and rigidity.

Based on the theoritical calculations and contructional evaluation, complete and individual CAD models of the tool and clamping device were also created. Additionally, an assembly of the tool and the clamping device was also made that included all the essential details starting from the technical drawings to the bill of materials (BOM). The assembly verified proper fit, and dimensional correctness of all the components.

In the next step, a finite element analysis (FEA) was performed on the tool and the clamping device assembly using ANSYS Workbench. The material chosen for the tool was HSS M2 with a yield strength of 2200 MPa. The results showed a maximum von Mises stress of 1318.5 MPa, which was under the yield strength limit of the chosen material. This result showed that the tool was within the safe limit of operation. Furthermore, a total deformation of 0.007 mm was also rcorded, which indicated high stiffness and elastic behaviour of the tool. In accordance with the theoretical expectations, stress and strain distributions exhibited bending-type deformation concentrated near the cutting edge.

To conclude, the results confirmed that the designed flat form tool and clamping device structurally makes sense, is dimensionally accurate, and is mechanically reliable for practical manufacturing applications. Its design would also ensure proper production repeatability to keep producing identical parts. Overall, the whole process serves as a reference for tool design and clamping system design in lathe-based manufacturing operations.

List of references/Bibliography

[1] Bodzás, S. (2023). GEOMETRIC ANALYSIS AND DESIGN OF FLAT FORM TOOLS. *Journal of Production Engineering*, *26*(1), 1–8. https://doi.org/10.24867/JPE-2023-01-001

[2] On My Toolings. In: Exploration of lathe form tools {online} https://onmytoolings.com/exploration-of-lathe-form-tools/ (Accessed 22.03.2025, 1:56 p.m.)

[3] Woodbury, R. S. (1963). *The Origins of the Lathe*. *208*(4), 132–143. https://doi.org/10.2307/24936538

[4] Know CNC. In: Who invented the lathe {online}

https://knowcnc.com/who-invented-the-lathe/ (Accessed 06.04.2025, 9:48 p.m.)

[5] Kamperidou, V., Barboutis, I., Vasiliki, K., & Ioannis, -barboutis. (2013). *Lathe Tool-It's Development from the Ancient times to Nowadays*. http://www.archimedesclock.gr/gr/kataskeves/diafora/tornos.html

[6] MachineMFG. In: What is a lathe? History and development {online} https://www.machinemfg.com/what-is-a-lathe-history-and-development/ (Accessed 06.04.2025, 10:06 p.m.)

[7] Madhusudhan M. (n.d.) *Concept of Lathe Machine and Welding Techniques*. Books Arcade, Delhi, India, 2023. p. 4–18. ISBN 978-81-19199-14-3.

[8] The Engineers Post. In: Types of lathe machines {online} https://www.theengineerspost.com/types-of-lathe-machines/ (Accessed 06.04.2025, 10:24 p.m.)

[9] Patel, H., & Chauhan, I. A. (2020). A Study on Types of Lathe Machine and Operations: Review. *International Journal of Advance Research and Innovation*, *8*(4), 84–86. https://doi.org/10.51976/ijari.842014

[10] The Engineers Post. In: Lathe machine operations {online} Lathe Machine Operations: Types and Techniques [with PDF] (Accessed 06.04.2025, 10:33 p.m.)

[11] On My Toolings. In: Carbide Lathe Form Tool {online} https://onmytoolings.com/lathe-cutting-inserts/carbide-lathe-form-tool/ (Accessed 22.03.2025, 11:20 p.m.)

[12] O'Hara, J., & Fang, F. (2019). Advances in micro cutting tool design and fabrication. In: *International Journal of Extreme Manufacturing* (Vol. 1, Issue 3). IOP Publishing Ltd. https://doi.org/10.1088/2631-7990/ab3e7f

[13] Ranganath, B.J. (2011). *Metal Cutting and Tool Design* (pp. 178-179, 183–190). Vikas Publishing House. https://books.google.hu/books?id=w4akDwAAQBAJ

[14] Indira Gandhi National Open University. (n.d.). *Design of forming tools*. (Unit 7, pp. 25–29).

[15] Mapa Tools Pvt. Ltd. In: *Flat Form Tools*. TradeIndia {online} www.tradeindia.com/products/flat-form-tools-c7266009.html (Accessed 16.04.2025, 11:53 p.m.)

[16] IndiaMART. In: *Circular form tools* {online}

https://www.indiamart.com/proddetail/circular-form-tools-19590024791.html (Accessed 17.04.2025, 12:03 a.m.)

[17] INTRAN. In: What is end forming? {online}

What Is End Forming? | Intran (Accessed 06.04.2025, 10:33 a.m.)

[18] Lomar Machine & Tool. In: *Endform tooling* {online}

https://lomar.com/products-equipment/endforming/tooling/endform-tooling/ (Accessed 17.04.2025, 12:15 a.m.)

[19] Bodzás, S. (n.d). *Design of Clamping Devices* [PDF document]. Unpublished manuscript.

[20] Carr Lane Manufacturing Co. In: Locating and clamping principles {online} Locating & Clamping Principles for Jig & Fixture Design | Carr Lane Mfg. (Accessed 06.04.2025, 10:55 a.m.).

[21] Cakir, M. C., & Isik, Y. (2005). Finite element analysis of cutting tools prior to fracture in hard turning operations. *Materials and Design*, *26*(2), 105–112. https://doi.org/10.1016/j.matdes.2004.05.018

[22] Obispo, S. L., & Chan, C. D. (2004). *EFFECTS OF TOOL GEOMETRY ON THE VIBRATIONS GENERATED IN CUTTING OPERATIONS ON A LATHE A Master's Thesis In Partial Fulfillment of the Requirements for the Degree Master of Science in Industrial Engineering*.

[23] Duran, A., & Nalbant, M. (2005). Finite element analysis of bending occurring while cutting with high speed steel lathe cutting tools. *Materials and Design*, *26*(6), 549–554. https://doi.org/10.1016/j.matdes.2004.07.028

[24] Özel, T., & Zeren, E. (2005). Finite element method simulation of machining of AISI 1045 steel with a round edge cutting tool. In: *Proceedings of*

the CIRP International Workshop on Modeling of Machining Operations. Rutgers University, USA. https://doi.org/10.13140/RG.2.1.1121.2006

[25] Kumari, L., Shaik, I. S., & Kumar, G. P. (2015). Analysis of single point cutting tool of a lathe machine using FEA. In: *International Journal of Engineering Trends and Technology* (Vol. 20, Issue 5). IJETT Publications. https://doi.org/10.14445/22315381/IJETT-V20P241

[26] Bodzás, S. (n.d). *Design of Flat Form Tools* [PDF document]. Unpublished manuscript.

[27] JAT Carbide. (n.d.). In: Feed rates and cutting speeds in machining {online} Feed Rates and Cutting Speeds in Machining - Jat Carbide (Accessed 19.11.2025, 2:28 p.m.).

[28] Machining Doctor. In: Specific Cutting Force (KC & KC1){online} Specific Cutting Force (KC & KC1) - Machining Doctor (Accessed 19.11.2025, 2:52 p.m.).

[29] AZO Materials. In: M2 Molybdenum High Speed Tool Steel (UNS T11302){online M2 Molybdenum High Speed Tool Steel (UNS T11302) (Accessed 19.11.2025, 4:21 p.m.).

[30] AZO Materials. In: AISI 4140 Alloy Steel{online} AISI 4140 Alloy Steel (UNS G41400) (Accessed 19.11.2025, 4:21 p.m.).

[31] Metal Zenith. In: 12.9 Alloy Steel: Properties and Key Applications {online} 12.9 Alloy Steel: Properties and Key Applications – Metal Zenith (Accessed 19.11.2025, 4:27 p.m.).